Unveil the unseen: Using LiDAR to capture time-lag dynamics in the herbaceous layer of European temperate forests

Jonathan Roger Michel Henri Lenoir, Eva Gril, Sylvie Durrieu, Helene Horen, Marianne Laslier, Jonas J. Lembrechts, Florian Zellweger, Samuel Alleaume, Boris Brasseur, Jerome Buridant, et al.

Journal of Ecology

Unveil the unseen: Using LiDAR to capture time-lag dynamics in the herbaceous layer of European temperate forests

Journal:	*Journal of Ecology*
Manuscript ID	JEcol-2021-0711.R1
Manuscript Type:	Review
Date Submitted by the Author:	n/a
Complete List of Authors:	Lenoir, Jonathan; CNRS Delegation Nord Pas-de-Calais et Picardie, Unité de Recherche "Ecologie et Dynamique des Systèmes Anthropisés" EDYSAN, UMR CNRS 7058 Gril, Eva; CNRS Delegation Nord Pas-de-Calais et Picardie, Unité de Recherche "Ecologie et Dynamique des Systèmes Anthropisés" EDYSAN, UMR CNRS 7058 Durrieu, Sylvie; TETIS Horen, Hélène; UPJV, Unité de Recherche "Ecologie et Dynamique des Systèmes Anthropisés" EDYSAN, UMR CNRS 7058 Laslier, Marianne; UPJV, Unité de Recherche "Ecologie et Dynamique des Systèmes Anthropisés" EDYSAN, UMR CNRS 7058 Lembrechts, Jonas; University of Antwerp, Biology Zellweger, Florian; WSL Alleaume, Samuel; TETIS Brasseur, Boris; UPJV, Unité de Recherche "Ecologie et Dynamique des Systèmes Anthropisés" EDYSAN, UMR CNRS 7058 Buridant, Jérôme; UPJV, Unité de Recherche "Ecologie et Dynamique des Systèmes Anthropisés" EDYSAN, UMR CNRS 7058 Dayal, Karun; TETIS De Frenne, Pieter; Ghent University, Forest & Nature Lab; Ghent University, Plant Production Gallet-Moron, Emilie; UPJV, Unité de Recherche "Ecologie et Dynamique des Systèmes Anthropisés" EDYSAN, UMR CNRS 7058 Marrec, Ronan; UPJV, Unité de Recherche "Ecologie et Dynamique des Systèmes Anthropisés" EDYSAN, UMR CNRS 7058 Meeussen, Camille; Ghent University Faculty of Bioscience Engineering, Department of Environment Rocchini, Duccio; Fondazione Edmund Mach, Biodiversity and Molecular Ecology Department, Research and Innovation Centre Van Meerbeek, Koenraad; KU Leuven, Department of Earth and Environmental Sciences Decocq, Guillaume; UPJV, Unité de Recherche "Ecologie et Dynamique des Systèmes Anthropisés" EDYSAN, UMR CNRS 7058
Key-words:	Historical ecology, Remote sensing, Time-lag dynamics, Understory layer, Archaeology, Legacy effects, Biodiversity, Climate change, Nitrogen deposition, Microclimate

Note: The following files were submitted by the author for peer review, but cannot be converted to PDF. You must view these files (e.g. movies) online.
Figure_1.svg Figure_5.tif Figure_6.tif

Article type: Essay Review submitted for the Grime Reviews series

Unveil the unseen: Using LiDAR to capture time-lag dynamics in the herbaceous layer of European temperate forests

Preliminary author list

Jonathan Lenoir[1], Eva Gril[1], Sylvie Durrieu[2], Hélène Horen[1], Marianne Laslier[1], Jonas Lembrechts[3], Florian Zellweger[4], Samuel Alleaume[2], Boris Brasseur[1], Jérôme Buridant[1], Karun Dayal[2], Pieter De Frenne[5], Emilie Gallet-Moron[1], Ronan Marrec[1], Camille Meeussen[5], Duccio Rocchini[6,7], Koenraad Van Meerbeek[8], Guillaume Decocq[1]

Affiliations

[1]Ecologie et Dynamique des Systèmes Anthropisés (EDYSAN, UMR 7058 CNRS), Université de Picardie Jules Verne, 1 rue des Louvels, 80000 Amiens, France

[2]UMR TETIS, Univ Montpellier, AgroParisTech, CIRAD, CNRS, INRAE, Montpellier, France

[3]Centre of Excellence on Plants and Ecosystems, University of Antwerp, Belgium

[4]Institut fédéral de recherches sur la forêt, la neige et le paysage WSL, Zürcherstrasse 111, 8903 Birmensdorf, Suisse

[5]Forest & Nature Lab, Ghent University, Geraardsbergsesteenweg 267, 9000 Gent, Belgium

[6]BIOME Lab, Department of Biological, Geological and Environmental Sciences, Alma Mater Studiorum University of Bologna, via Irnerio 42, 40126, Bologna, Italy

[7]Czech University of Life Sciences Prague, Faculty of Environmental Sciences, Department of Spatial Sciences, Kamýcka 129, Praha-Suchdol, 16500, Czech Republic

[8]Department of Earth and Environmental Sciences, Division Forest, Nature and Landscape, KU Leuven, Belgium

Abstract

1. To understand time-lag dynamics in the response of biodiversity to macro-environmental changes (e.g., macroclimate warming and atmospheric pollution), we need to consider other anthropogenic forcing factors such as land-use changes and changes in management practices that can have both compounding and confounding effects. This is especially true in European temperate forests, where legacies from past human activities have left strong imprints on today's understory plant species composition, generating long-term lagging effects which can be mistakenly attributed to more recent macro-environmental changes.
2. By combining the expertise of plant, soil, and historical ecologists together with remote sensing scientists, we review the potential of light detection and ranging (LiDAR) to unveil ghosts from the past in terms of former land uses and management practices.
3. We show that imprints from past land uses and management practices can still be captured today throughout well-chosen LiDAR-derived variables describing, at sub-decimetre scale, the vertical and horizontal micro-variations of vegetation and terrain structure hidden below treetops.
4. *Synthesis*. We encourage plant and soil ecologists to use LiDAR data and to work with historians, archaeologists, and remote sensing scientists in order to select meaningful LiDAR-derived variables to account for time-lagged biotic responses to long-term macro-environmental changes.

Keywords

Archaeology, biodiversity, climate change, climatic debt, disequilibrium dynamics, forest management, historical ecology, legacy effects, microclimate, nitrogen deposition, remote sensing, understory layer

"When light encounters a strong magical field it loses all sense of urgency. It slows right down." – Terry Pratchett, The Light Fantastic (1986)

Introduction

The current warming of the climate system is unprecedented in terms of its speed and spatial extent within the context of the past 2,000 years (Neukom et al., 2019), leading to important regional, continental, and global biodiversity changes: species range shifts (Lenoir et al., 2020); shifts in the phenological synchrony of species interactions (Kharouba et al., 2018); community thermophilization (i.e., increasing dominance of warm-adapted species) (Gottfried et al., 2012); biotic homogenization (Staude et al., 2020); and even species extinction (Panetta et al., 2018). Yet, the velocity at which these biotic responses happen is generally lower than the velocity at which the macroclimate is warming (Bertrand et al., 2011; Dullinger et al., 2012; Rumpf et al., 2019; Vitasse et al., 2021), leading to disequilibrium or lagging dynamics (Alexander et al., 2018; Svenning & Sandel, 2013) sometimes also referred as the (macro)climatic debt in the scientific literature (Bertrand et al., 2016; Devictor et al., 2012; Richard et al., 2021). Likewise, delayed recovery of plant species richness and composition in response to the decreased inputs of atmospheric pollutants, after the peak in Europe during the 1970s for sulphur and during the 1980s for nitrogen, have been reported for both forest and grassland habitats (Riofrío-Dillon et al., 2012; Storkey et al., 2015).

Lagging dynamics in response to macroclimate warming and the reduction in atmospheric deposition, among other macro-environmental change drivers, are especially pronounced within the herbaceous layer of temperate deciduous forests (Bertrand et al., 2011, 2016; De Frenne et al., 2013; Richard et al., 2021; Riofrío-Dillon et al., 2012; van Dobben & de Vries, 2017), which is the most biodiversity-rich vegetation layer in these ecosystems (Gilliam, 2007; Landuyt et al., 2019). In terms of biotic responses to macroclimate warming, thermophilization rates are ranging from 0.01

to 0.05°C per decade within understory plant communities of temperate forests, which is several orders of magnitude lower (cf. greater lags) than the rates observed in other groups such as trees (0.11°C per decade), bumblebees (0.14°C per decade), freshwater invertebrates (up to 0.22°C per decade), or marine fishes and invertebrates (up to 0.38°C per decade) (see Table S5 in Richard et al. (2021), and references therein, for a more exhaustive description). For comparative purposes, mean annual temperature increased at a rate of 0.23°C per decade between 1995 and 2015 in France (Richard et al., 2021). As for the recovery time following the reduction in atmospheric deposition in Europe, lagging effects seem also more pronounced in the herbaceous layer of forests than in grassland communities (Schmitz et al., 2019; Storkey et al., 2015; van Dobben & de Vries, 2017). However, whether or not the magnitude of these time-lagged biotic responses in temperate forests can be attributed solely to macroclimatic warming or atmospheric deposition remains an open question. To resolve this, it is of utmost importance to also consider other anthropogenic forcing factors such as past land-use changes and historical changes in forest management practices that can have both compounding and confounding effects with other more recent environmental change drivers (Forister et al., 2010; Guo et al., 2018; Larsen, 2012; Warren et al., 2001). Indeed, the scientific literature is full of examples, detailed below, illustrating how the history of forest management practices and land uses can interact, synergistically or antagonistically, with either macroclimate warming or atmospheric deposition, to delay or sometimes speedup changes in the understory of European temperate forests.

As macroclimate warming accelerates, it is assumed that mean annual temperatures below treetops increase as well but at lower rates than outside forests due to the lower coupling between macroclimate and microclimate inside the forest understory (Lenoir et al., 2017). Accordingly, De Lombaerde et al. (2021) predicted that maximum temperatures will, on average for the 2060-2080 period, warm less inside (+0.27°C) than outside (+0.60°C) forests if the local forest cover is maintained. However, maximum temperatures may also warm faster inside the

93 forest understory than outside if canopy cover is reduced due to, for instance, management
94 interventions or forest dieback related to drought and pest damages. Such forest microclimate
95 dynamics driven by changes in canopy cover could explain part of what seems to be a delayed
96 biotic response to macroclimate warming, meaning that the so-called macroclimatic debt involves
97 microclimatic processes (De Frenne et al., 2021; Zellweger et al., 2020). Accordingly, Richard et al.
98 (2021) have recently demonstrated that lags in community thermophilization are accumulating
99 over time in the herbaceous layer of denser and older forest stands in France, while anthropogenic
100 and natural disturbances generating canopy gaps above the herbaceous layer tended to reduce
101 these lags. Hence, stand characteristics are important determinants of time-lag dynamics
102 observed in the herbaceous layer of temperate forests in response to macroclimate warming
103 (Brice et al., 2019; Richard et al., 2021). Besides, changes in stand characteristics over time interact
104 with long-term environmental changes through complex historical trajectories of forest
105 management practices and natural disturbances (e.g., fire, drought, wind storm). For instance, in
106 Europe, Perring et al. (2018) have shown that the trajectories of changes in forest plant
107 community composition over 40 years were clearly influenced by complex interactions between
108 management legacies from over 200 years ago and long-term environmental changes, in terms of
109 both the rate of nitrogen deposition and the rate of temperature change.

110 Time-lagged biotic responses that we attribute today to macroclimatic warming or to the
111 reduction in atmospheric deposition may also involve other long-term processes, such as legacy
112 effects of soil compaction due to mechanized timber harvesting as well as more ancient legacy
113 effects of past land uses (Bürgi et al., 2017), operating through microclimate and soil memory
114 effects. For instance, it has been recently demonstrated that old skid trails left by forestry vehicles
115 more than 50 years ago locally increase soil compaction and alter microclimatic conditions in the
116 soil (humidity and temperature), which leaves a strong imprint on contemporary community
117 composition and diversity in the herbaceous layer of temperate forests (Wei et al., 2015). More

precisely, by limiting water infiltration, skid trails locally increase the proportion of wetland plant species in the community (Buckley et al., 2003), which alters community composition such that the community may not only indicate wetter but also cooler conditions over time when analysed through the lens of thermophilization indices solely. Indeed, a cooling effect is usually concomitant with the humidifying effect of vegetation (Zhang et al., 2013). In such a case, time-lagged biotic responses to soil compaction by skid trail may be mistakenly attributed to an inflated macroclimatic debt.

The field of historical ecology (Szabó, 2015) is full of examples showing that current local biodiversity continues to be influenced by past management practices and land uses, including fire regimes, through complex biotic lags usually involving long-lasting effects of changes (or absence of changes) in landscape configuration and soil abiotic conditions (Dambrine et al., 2007; Dupouey et al., 2002; Jung et al., 2019; Metzger et al., 2009). For instance, time since afforestation, and thus land-use history, has left a strong imprint on the herbaceous layer of temperate deciduous forests in Europe, with several forest plant species (i.e., forest specialists) clearly associated with ancient forests (land continuously forested for several centuries) (Rackham, 2008) as opposed to more recent forests (Hermy et al., 1999; Peterken & Game, 1984; Valdés et al., 2015; Verheyen et al., 2003). Similarly, historical landscape connectivity can strongly affect the present distribution pattern of herbaceous forest plants in fragmented forests and hedgerows through changes in habitat configuration and composition (Lenoir et al., 2021; Lindborg & Eriksson, 2004; Metzger et al., 2009). Perhaps more surprisingly, former Roman agricultural practices throughout Europe can still have irreversible impacts on forest biogeochemical cycles and biodiversity by increasing today's soil pH, available phosphorus and nitrogen, and consequently the frequency of nitrogen-demanding species (Dambrine et al., 2007; Plue et al., 2008; Vanwalleghem et al., 2004). In such a case, without considering historical information on past land uses, one may mistakenly interpret todays' occurrence of nitrogen-demanding species in the community as a response to the high

nitrogen deposition during the 1980s while part of it may actually be due to longer-term lagging effects induced by former Roman agricultural practices. By looking at terrain morphology and micro-topographic variations in today's landscapes, archaeologists and geo-historians can read such long-term legacies from past land uses, unearth artefacts of former human occupations, and provide invaluable information to explain current biodiversity patterns (Briggs et al., 2006; Closset-Kopp & Decocq, 2015; Dambrine et al., 2007; Dupouey et al., 2002; Plue et al., 2008). Hence, to decipher the main determinants of time-lag dynamics in the herbaceous layer of temperate forests it is necessary to analyse the response of species population and community dynamics to contemporary macro-environmental changes (e.g., macroclimate warming or nitrogen deposition) in the light of historical management practices and past land uses.

Vertical and horizontal micro-variations at sub-decimetre scale in both vegetation and terrain structure can bear the imprints of historical management practices and land-use legacies which are still contributing to today's biodiversity, and thus to time-lagged biotic responses to macro-environmental changes, by locally altering microclimatic conditions near the soil surface as well as edaphic conditions (**Fig. 1**). Light detection and ranging (LiDAR) data (**Box 1**) can capture these vertical and horizontal micro-variations (i.e., structural traits) below treetops (**Fig. 2**). Indeed, LiDAR data can provide quantitative metrics of both stand characteristics and micro-topographic variations below the canopy at unprecedented detail, often impossible to perceive for the human eye or to describe with traditional field measurement methods (Chase et al., 2012; Dassot et al., 2011). To illustrate this, we first put on our plant-ecologist hat to show how LiDAR data can capture detailed stand characteristics to unveil recent but also historical forest management practices that affect current forest microclimates and thus the time-lag dynamics of understory plants' responses to long-term environmental changes. Then, we put on our soil-ecologist hat to illustrate how LiDAR data can unveil the imprints of former skid trails left by forestry vehicles that are still affecting current plant community composition through soil compaction. Third, we take a

historical-ecologist viewpoint to demonstrate how LiDAR data can unveil long-term land use history that may still affect contemporary plant community composition in the herbaceous layer. Finally, we discuss research perspectives in light of the most recent advances in LiDAR technology and its combination with other remote sensing technologies as well as with recent developments in computer science. We conclude that LiDAR can be used as a tool to boost trans-disciplinary research between plant ecologists, foresters, soil ecologists, archaeologists, historical ecologists, and remote sensing scientists to advance our knowledge of time lags in the response of understory plant communities to long-term macro-environmental changes.

Box 1: LiDAR principles

Measurement principles

Light detection and ranging (LiDAR) is an active remote-sensing technology based on emission-reception of a laser beam. LiDAR can be divided into two main categories (Durrieu et al., 2015; Grotti et al., 2020): (1) time-of-flight LiDAR (**Fig. 2**) assessing distances by measuring the roundtrip time for a short laser pulse, in general emitted by a near-infrared or visible (green) laser, to travel between the sensor and a target; versus (2) phase-shift LiDAR emitting a continuous wave laser with intensity modulated at a series of frequencies to determine distances through shifts in phase of the returned modulations. Phase-shift LiDAR have higher measurement rates and can thus collect data at a much faster speed than time-of-flight LiDAR. They also measure distance with a precision of up to few millimetres against few centimetres for time-of-flight LiDAR. However, their maximum measurement range is much shorter, which makes phase-shift LiDAR more adapted for terrestrial LiDAR systems (TLS) than for airborne LiDAR systems (ALS) (**Fig. 2**). Additionally, phase-shift LiDAR is more prone to artefacts, for example those caused by range averaging, when a beam partially intercepts more than one object.

Scanning and geolocating principles

In order to acquire LiDAR data across a given area or landscape, a scanning system is used to deflect the emitted laser beams in different directions throughout the target scenery (**Fig. 2**). This is achieved thanks to: (1) the combination of a moving (e.g., rotating) mirror and the movement of either the scan head for static TLS or the vehicle on which the LiDAR is embedded for non-stationary systems like ALS (Tan et al., 2018); and (2) the multiplication of standpoints for TLS or flight lines for ALS. When both the scanning angles and the position of the LiDAR in a geographic reference system are known at the time of range measurements, the absolute position of the targets on the Earth's surface can be inferred. For mobile ALS, real-time sensor position and

orientation are obtained thanks to a differential global navigation satellite system (DGNSS) and an inertial measurement unit on-board the platform. For static TLS, point cloud geolocation can be achieved by measuring either scan positions or the positions of a set of high reflective targets distributed in the field, which are clearly identifiable in the point clouds and used for the merging of several scans. Positions can again be measured using a DGNSS. To improve location accuracy in forest environments, it is recommended to use a DGNSS in a neighbouring open area as well or coupled with a total station (cf. tacheometer).

Spatial distribution of LiDAR measurements and occlusions

The spatial distribution of LiDAR measurements results from the combination of several factors, such as laser emission rate, scanning system, and vector velocity for non-stationary ALS. However, a major phenomenon impacts the spatial distribution of LiDAR measurements in forested environments: occlusions. Like natural light, laser beams can penetrate through vegetation openings but, when intercepted by vegetation elements, it is mostly reflected or absorbed, generating shadows or occluded areas behind these elements (e.g., foliage, stems, flowers). Besides, the quantity of light continuing its path through vegetation decreases each time part of a laser beam hits a vegetation element. As a result, vegetation sampling is getting sparser when the laser beam goes deeper inside the vegetation (**Fig. 2**). For TLS, point density decreases with the distance from scan positions below the canopy, leading to sparser point clouds towards the top of the canopy and generating occlusion areas behind large tree trunks located very close to the scanning position. For ALS, the understory vegetation and the ground surface, including deadwood and litter lying on the ground, are less densely measured than the top of the canopy, especially after leaf-out and tree canopy closure in temperate deciduous forests.

Using LiDAR-derived metrics of vegetation structure to capture time-lag dynamics in the response of herbaceous plant communities to long-term environmental changes

Forest structure is acknowledged to be a key factor to explain current plant species diversity and community composition in the understory (Oettel & Lapin, 2021; Walter et al., 2021). LiDAR technology allows the description of complex aspects of the forest structure that are complementary to those observed by foresters during field surveys (**Box 2**) (Bouvier et al., 2015; Venier et al., 2019). Primarily underpinned by objectives of forest resource inventory and management, the capacity to remotely assess stand characteristics such as basal area, stem density, dominant height, wood volume, and biomass distribution, has been widely studied and is operationalized in a variety of forest contexts (Moeslund et al., 2019; White et al., 2016; Wulder et al., 2013). Among those descriptors of stand attributes routinely used by foresters to assess forest resources, some, like stand structure (e.g., basal area, diameter diversity, tree height), management intensity, and tree species composition have proven to be useful to model current plant diversity in the forest understory (Oettel & Lapin, 2021; Wei et al., 2020). However, many other complementary metrics (e.g., canopy volume, vertical leaf density profile, understory shrub cover), not routinely used by foresters to assess vegetation structure because they are difficult to measure in the field, can be derived from LiDAR data (**Fig. 3**). In this review, we argue that LiDAR data can be used to derive variables describing the complexity of the vertical layering of vegetation in temperate forests, including subtle vertical structures bearing the imprints of extreme weather conditions as well as the memory of past forest management practices for which we have good records in Europe.

It is widely acknowledged that historical forest management practices, such as coppicing which was widespread in European temperate forests before World War II (WWII), are major drivers of current plant community composition and distribution in the forest understory (Bartha et al.,

2008; Becker et al., 2017a; Bricca et al., 2020; Decocq et al., 2004; Della Longa et al., 2020; Müllerová et al., 2015). For instance, former coppice-with-standards (CWS) have left a visible signature on current stand structure as well as on current plant species composition in the herbaceous layer, even after conversion to high forests (HF), a very common practice in Europe after WWII. Importantly, these changes in forest management practices in Europe happened somewhat concomitantly with climate change and increased inputs of nitrogen via atmospheric deposition, leading to complex compounding and confounding effects on the observed changes in plant species composition in the herbaceous layer (Becker et al., 2017b; Perring et al., 2018). Traditionally, CWS were managed as multi-storied stands consisting of a matrix of even-aged stems (coppice) in the lower storey – cut down for firewood production in short rotations – and single-stem (emergent) trees (i.e., standards) in the upper storey – left standing during longer rotations for timber production. Whether or not CWS casts more shade at the forest floor than HF remains unclear, but conversion from CWS to HF implies more regular thinning operations over time, potentially leading to more frequent light pulses enhancing microclimate warming and community thermophilization in the understory, ultimately compounding and confounding the impact of macroclimate warming on understory plant communities (Zellweger et al., 2020). Changing socio-economic conditions throughout history have also led to the complete abandonment of active timber management in some regions of Europe (see Perring et al., 2018), generating prolonged absence of high light conditions in the forest understory. Such trajectories may have led to a loss of light-demanding plant species from open habitats and an increase of typical shade-tolerant plant species (i.e., forest specialists) (Baeten et al., 2009), reducing community thermophilization and contributing to the lagging response of understory forest plant to macroclimate warming (Richard et al., 2021).

Using LiDAR technology to scan the vertical layering of vegetation and better capture the understory structure hidden below treetops (**Box 2**), as a mean to identify the complex trajectories

outlined above, holds untapped potential to understand time-lag dynamics that depends upon past management legacies (Perring et al., 2018). For instance, a set of airborne LiDAR-derived variables describing the vertical distribution of canopy height and cover was successfully applied to identify old coppices in a Mediterranean context (Bottalico et al., 2014). The most straightforward metrics to describe the vertical structure of vegetation within a given spatial grid cell include the mean and standard deviation of height values above the ground surface for all the points classified as vegetation and belonging to the focal grid cell. Yet, these raw summary statistics aggregated in a 2D pixelated space may not fully capture the complex layering of vegetation in the understory (see **Box 2**). Refined approaches to assess the effective number of vegetation layers below treetops consist in computing height percentiles and the number of echoes or point density at several heights (Frey et al., 2016; Stickley & Fraterrigo, 2021). Using airborne LiDAR data, Stickley & Fraterrigo (2021) summarized the vertical structure of temperate deciduous forests in the Great Smoky Mountains National Park into five height classes and found that variation in maximum temperature in the understory was best explained by the buffering effects of the low-understory (below 5 m height) and low-canopy (from 10 to 15 m height) layers. Finally, it is possible to compute more advanced LiDAR-derived metrics per unit of volume (see **Box 2**) by relying on the resolution of the transmittance equation using the Beer-Lambert Law, which relates the attenuation of light through a turbid medium – in this case, leaves and branches – to the properties of that medium, or on the maximum likelihood theory (Soma et al., 2018). For instance, plant area density (PAD) (in $m^2\ m^{-3}$) can first be computed for each single voxel, a 3D cell unit, from the local transmittance values by applying Beer-Lambert's turbid medium approximation (Vincent et al., 2017) (**Fig. 3e**). Thus, PAD values better reflect the amount of plant material participating to light occlusion in the canopy than the above-mentioned metrics based on point density. From vertical profiles of PAD values (**Fig. 3f**), it is then possible to summarize the entire vertical structure of vegetation, including the understory, by computing the plant area index

(PAI), which is the integral (area under the curve) of PAD profiles. Hence, PAI describes the entire column of plant material participating to light occlusion and thus indirectly reflects the amount of light reaching the forest floor. **Figure 4** shows that a denser forest with a complex shrub layer and thus a higher PAI value (e.g., PAI = 6.28) than a less vertically complex and more open forest (e.g., PAI = 4.72) provides a higher buffering capacity during spring and summer, reducing daily mean temperature by more than 5°C (against 3°C for the open forest). It is also possible to compute PAI within a restricted vegetation layer, such as the shrub layer (e.g., below 7 m). This way, it is possible to partition PAI values among vegetation layers and focus on the additional insulating effect provided by shrubs (**Fig. 4**), which may bear the imprints of historical management practices contributing to time-lag dynamics in the herbaceous layer. Spatially contiguous maps of forest microclimate predictions (e.g., Frey et al., 2016; George et al., 2015) integrating the buffering effects of the understory shrub layer through the use of PAI values are especially promising as they may reflect the complex trajectories of forest management changes, and explain time-lag dynamics in the response of the herbaceous layer to long-term environmental changes (Richard et al., 2021; Zellweger et al., 2020).

Box 2: The potential of LiDAR-derived variables to capture vertical structures in the understory

Traditional forest inventory methods to measure forest structure in the field cannot be easily applied contiguously at fine spatial resolutions and across large spatial extents. Moreover, traditional forest surveys cannot extract the accurate three-dimensional structure of forests, including tree cover rate, gap distribution, and a detailed vertical description of the understory. Using LiDAR data can help to overcome these limitations (Almeida et al., 2019) (**Fig. 3**). Once the digital terrain model (DTM) (**Fig. 3a**) of a given area has been computed from the set of points classified as "ground", it is possible to compute the exact height, relative to the ground surface, of each point classified as "vegetation" across the area. This information can then be exploited to extract very simple metrics of the vertical structure of vegetation, such as canopy density above a specific height (**Fig. 3b**) or maximum canopy height (**Fig. 3c**). The level of details provided by LiDAR data, and especially TLS data (**Figs. 3d**), to quantitatively describe the vertical layering of vegetation in the understory of temperate forests (**Fig. 3e,f**) is unprecedented compared to traditional field approaches (Venier et al., 2019). Foresters usually start recording and measuring trees in the field above a minimum diameter at breast height (DHB) of 7.5 cm. Yet, individuals of less than 7.5 cm DBH are also an important component of the understory shrub layer that can be partly captured depending on the quality of the raw LiDAR point cloud. The quality not only depends on the point density, which can be high in case of TLS data (**Fig. 3d-f**), but also on the intensity of the return and the number of echoes registered. For ALS data, full-waveform laser scanning allows to digitize the complete waveform of each backscattered pulse and extract more small echoes – even during leaf-on conditions – that may hold key information on the structure of the understory shrub layer. From the raw LiDAR point cloud, the most intuitive approach to capture the understory shrub layer is to separate points classified as "vegetation" into different vertical strata and extract summary statistics aggregated in a 2D pixelated space describing either

the mean, minimum, maximum, standard deviation, skewness, kurtosis, or relative percentage of the distribution of the points within a vertical stratum (e.g., Frey et al., 2016; Stickley & Fraterrigo, 2021). To avoid using too many summary statistics for each vertical layer separately, LiDAR point clouds classified as vegetation can also be aggregated in a 3D voxelated space to compute metrics per unit of volume, like the 3D distribution of plant or leaf area density (PAD or LAD) (**Fig. 3e**). For instance, Almeida et al. (2019) showed that LAD profiles have the capacity to track changes in forest structure under different forest management practices. This biophysical information can be further analysed to provide vertical vegetation profiles or information on gap size and distribution (**Fig. 3f**). Vertical profiles and gap fraction together can better describe the 3D characteristics of the forest. Venier et al. (2019) identified several metrics that are expected to directly capture vegetation density in the understory: fractional cover (FRAC); plant or leaf area density (PAD or LAD) profiles; voxel cover (VOX); and normalized cover (NORM). Additionally, the Gini coefficient is a reliable descriptor of variation in tree sizes (Knox et al., 1989). Valbuena et al. (2016) demonstrated the potential of LiDAR-derived estimations of the Gini coefficient to highlight structural differences between forests that have been protected since the beginning of the 20th century *vs*. forests presently under intense management.

Using LiDAR data to highlight soil compaction from skid trails affecting current biodiversity patterns in the forest understory

Numerous studies have highlighted the long-lasting effects of heavy forestry vehicles on soil processes and forest herb composition (Closset-Kopp et al., 2019; Godefroid & Koedam, 2004; Wei et al., 2015). These effects include: (i) diaspore dispersal via the mud attached to tires and wheels (i.e., agestochory) and air displacement induced by the vehicle's movements, which facilitates anemochory; (ii) the creation of microreliefs within, beside, and between wheel tracks, generating a complex mosaic of microenvironments; and (iii) local changes in soil abiotic (e.g., porosity, microclimate, chemistry) and biotic (e.g., microbial activity) conditions. In particular, soil compaction and the formation of deep ruts on the soil surface often impede water infiltration, oxygen supply, nutrient bioavailability, as well as root development (Arocena, 2000; Cambi et al., 2018; Kozlowski, 1999). This provides regeneration niches and suitable habitat conditions to a range of (non-forest) plant species, such as aquatic weeds, sedges and rushes, as well as ferns (Closset-Kopp et al., 2019) but on the other hand can negatively affect recruitment of other species (e.g., trees). These three processes can lead to an increase in local species richness, yet also a process of homogenization among forest habitats, by facilitating the colonization of the same suite of wetland and ruderal species (Closset-Kopp et al., 2019; Godefroid & Koedam, 2004; Kozlowski, 1999).

Ruts and soil compaction can be measured in the field, via rut depth, bulk density, or penetration resistance, but the methods are time consuming to apply across large areas. Recently, several studies highlighted the efficiency of remote sensing in the evaluation of rutting intensity and spatial distribution (Marra et al., 2018; Mohieddinne et al., 2019; Niemi et al., 2017). Some of them, using unmanned aerial vehicles equipped with digital cameras for high resolution photogrammetry, returned a fine description of rut density associated with forest harvesting

(Marra et al., 2018; Talbot et al., 2018). However, this approach is only applicable to recently clear-cut areas. In contrast, LiDAR data offers an interesting alternative to map skid trails below treetops (**Fig. 5**) (Koren et al., 2015; Mohieddinne et al., 2019; Niemi et al., 2017). Indeed, points classified as "ground" in the LiDAR point cloud can be used to generate a digital terrain model (DTM) at sub-decimetre resolution so as to detect microrelief variations due to skid trails. The most straightforward approach to highlight skid trails from a DTM is to use local relief models (LRMs) that are widely used in archaeology to capture local, small-scale elevation differences after removing the large-scale landscape forms from the data (Hesse, 2010). While TLS data can yield LRMs at a very high accuracy over limited spatial extents (Koren et al., 2015), ALS data allows assessing the impact of skid trails over much larger areas in a spatially contiguous manner (Niemi et al., 2017). **Figure 5** clearly shows how ALS data can shed light on skid trails in the Compiegne forest, a managed state forest in Northern France. The LRM reveals small-scale topographic variations such as ruts, which sometimes appear as parallel paths following permanent skid trails as delineated by forest managers (**Fig. 5a**, bottom panels) but also as numerous meandering paths crossing each other (**Fig. 5b**, bottom panel). Yet, LRMs only highlight ruts resulting from the traffic intensity without providing the means for an automatic detection of these linear small-scale topographic elements in the landscape. Indeed, one still needs to digitize, manually, the illuminated ruts in the LRM image in order to analyse these elements afterwards. By doing so across the entire Compiegne forest, we found that the surface area covered by skid trails can reach 40 to 80% in several of the forest management units. Noteworthy, in some of these units, many ruts intersect (**Fig. 5b**). This suggests that either vehicles travel unevenly during a given operation or that older ruts resulting from several successive forestry operations persist for a very long time (at least 50 years) (Ebeling et al., 2016; Mohieddinne et al., 2019) with potential long-lasting effects still visible on today's plant species composition and diversity in the herbaceous layer (Wei et al., 2015). More specifically, the cumulated effect of soil compaction due to repeated

traffic of heavy forest harvesters and forwarders contribute to local increases in the proportion of wetland plant species in the community (Buckley et al., 2003) and to the homogenization of plant communities in the forest understory (Closset-Kopp et al., 2019), most likely with a lagging effect. Without considering skid trails, such time-lag dynamics can be misattributed to other concomitant drivers of change in environmental conditions, such as nitrogen deposition known for being also responsible for the biotic homogenisation of understory plant communities (Staude et al., 2020). Currently, the main challenge to account for the impact of skid trails on understory vegetation at large spatial extents is to automatize the detection of ruts from LRM images. More research is still needed to achieve that but one possibility is to train a model with LRM data using machine learning or deep learning algorithms such as convolutional neural networks (CNNs), which is widely used in the field of computer vision (Ren et al., 2017).

Using LiDAR data to unveil past land uses affecting current biodiversity patterns in the forest understory

One leading research question in historical ecology is (Plue et al., 2009): what did past human societies leave behind and how does this influence present ecosystem functioning? For ecologists, this question can be difficult to answer without a comprehensive knowledge of past interactions between human societies and the environment at various spatial and temporal scales. LiDAR technology has prompted an "archaeological revolution" by making it possible to identify, map, and analyse hidden objects and structures (Costa et al., 2020; Hesse, 2010). In terms of historical ecology, this is especially true for forested lands, where traditional remote sensing techniques such as aerial photography cannot unveil archaeological features hidden below treetops. In such situations, ALS can help to spot thousands of artefacts in a much shorter time frame than the decades of pedestrian field surveys that would have been otherwise necessary to discover only the most visible part of these artefacts (Chase et al., 2012; Štular et al., 2021). In many cases, ALS has revealed previously unrecorded archaeological features. Spectacular examples of unexpected findings are the medieval landscape planning by the classical Khmer civilization at Angkor (Evans et al., 2013) and the early Maya metropolises in Guatemala (Canuto et al., 2018) and Mexico (Inomata et al., 2020). Recent advances in deep learning algorithms may even allow to automatize the inventory of archaeological remains (Oliveira et al., 2021; Trier et al., 2021). For instance, Oliveira et al. (2021) applied CNNs on ALS data to automatically detect charcoal kilns dating back to the industrial development period (17th-19th century) in North-eastern France. However, remote and automatic detection still requires confirmation, either by field observations or through the experienced eyes of archaeologists and geo-historians who can read and interpret images processed from LiDAR data.

In Western Europe, many big woodlands have been continuously mapped or mentioned in archives since the Middle Ages, so that they have long been considered as relicts of prehistoric forests (Maury, 1850). This hypothesis was first challenged by the discovery of former Roman settlements in these forests (Cauchemé, 1912; Desbordes, 1973; Laffite et al., 2002) and it is now largely invalidated by ALS data which has revealed that these ancient forests were established on former agricultural lands, often intensively cultivated during the Middle Ages and Antiquity (**Fig. 6**) (Fruchart, 2020; Georges-Leroy et al., 2011; Rassat & Hugonnier, 2017). **Figure 6** illustrates this phenomenon by unveiling past land uses hidden below treetops of the Compiègne forest in Northern France, questioning the existence of prehistoric forest remnants in the Gallo-Roman lowlands. With the increasing amount of land covered by ALS data (Fruchart, 2020), it becomes obvious that what we today consider to be very ancient forests can result from recolonization of abandoned Roman farmlands (Georges-Leroy et al., 2011). Also in Eastern Europe, ALS unveiled more than 300 km of field boundaries and many (pre-)Roman settlements in the iconic “primary” forest of Bialowieza in Poland, indicating that the present forest has largely established on former Celtic, Roman, and medieval fields, towards the 13th century AD (Stereńczak et al., 2020). Beyond the reconstruction of the past landscapes, ALS renders it possible to assess the impact of past land uses on current vegetation patterns and ecosystem processes. For example, buried former Roman settlements typically host a species-rich, nitrogen-demanding understory, which often strongly contrasts with the surrounding species-poor, acidophilous forest vegetation (Dambrine et al., 2007; Dupouey et al., 2002; Plue et al., 2008). Interestingly, the soil seed bank in the Compiègne forest indicates that plant communities associated with these former settlements can self-perpetuate over time (Plue et al., 2008). This has been related to long-lasting alterations of biogeochemical cycles, which extend far beyond the settlement, thereby creating strong ecological gradients with different species assemblages (Dambrine et al., 2007).

Airborne LiDAR data also revealed the recurrence of certain human artefacts, even outside ancient settlements located in formerly cultivated land, and highlight their possible ecological significance in forests. We hereafter give three examples. Firstly, in North-eastern France, closed depressions found on calcareous substratum have long been supposed to be of natural origin, but archaeological research has suggested that they were rather artificial excavations from the late Iron Age and Roman times, used to (i) extract marls (i.e., calcium carbonate or lime-rich mud) to amend agricultural lands and/or to (ii) create local depression to collect water for livestock (Etienne et al., 2011). Since this early publication, similar closed depressions have been recorded thanks to ALS data in many "post-Roman" ancient forests elsewhere in Northern France (see **Fig. 6** for an illustration in the Compiègne forest), suggesting that liming was a common practice during Gallo-Roman times. Long-lasting effects on soil properties, plant communities, tree growth, and forest health are thus expected (Brasseur et al., 2018; Dambrine et al., 2007; Dupouey et al., 2002; Moore & Ouimet, 2021). For instance, the effect of ancient liming practices is still visible on today's soil pH profile of post-agricultural forests, albeit this effect diminishes with the age since afforestation (Brasseur et al., 2018). Being able to date the approximate age of the last agricultural practices before afforestation makes it possible to estimate the magnitude of the imprint left by former agricultural practices in the soil, and thus the effect on forest biodiversity and ecosystem processes. The last agricultural practices are precisely those that most impacted the microrelief preserved under the canopy of post-agricultural forests. Because of these microreliefs' imprints, geo-historians and archaeologists are able to read images from processed ALS data, such as a DTM with hillshade (**Fig. 6**), and interpret characteristic microreliefs to identify Middle Ages strip fields with cultivation ridges (**Fig. 6b**), Gallo-Roman linear agrarian fields (**Fig. 6c**), or even Celtic fields (Meylemans et al., 2015). The approximate age since afforestation as well as the type of former agricultural practices can be key explanatory variables to capture time-lag dynamics in the

response of understory plant communities to the acidification rates of afforested soils that were formerly cultivated (De Schrijver et al., 2012).

Secondly, another insight from ALS data is the evidence of an incredibly high density of former charcoal kilns (i.e., chambers or ovens to turn wood into choarcal) in several forests across Europe, from North-eastern France to Norway (Oliveira et al., 2021; Trier et al., 2021). This not only indicates the huge intensity at which European forests used to be managed from the Middle Ages to the end of the 19th century when humans started to mine and drill fossil fuels (Oliveira et al., 2021), often as short-rotation coppice woodlands, but also that soils have been considerably enriched in organic matter, carbon, and ash (Bonhage et al., 2020; Rutkiewicz et al., 2019). As a result, these former "charcoal-producing coppices", that are often managed as high forests nowadays, harbour different plant communities and soil properties compared to woodlands that have been continuously managed as high forests. For instance, the Bernadouze forest in the French Pyrenees was initially managed as a beech coppice with fir standard before being progressively transformed, during the 15th-17th century, into a monospecific beech coppice for charcoal production, inducing long lasting effects on today's biodiversity and soli processes (Fouédjeu et al., 2021). Charcoal-producing coppices may contain an additional 4.9 to 8.9 Mg ha^{-1} of soil carbon, and even more (Bonhage et al., 2020). In regions where former charcoal kilns were associated with metal furnaces to forge weapons during medieval times, it may further explain local soil pollution and its persisting effect on biodiversity and ecosystem processes (Karlsson et al., 2015).

Thirdly, still in the Compiègne forest, ALS data also unveiled a number of raised, circular structures that concentrated along a curved line into the forest, a few hundreds of meters from the current edge. Field surveys identified them as rabbit warrens, that are artificial earth clods, also called "mottes à conils" in French, erected at the end of the Middle Ages to rear rabbits for royal hunting

parties (Germond et al., 1988; Williamson, 2008; Zadora-Rio, 1986). This finding allows not only to date the introduction of rabbit in Northern France somewhere between the 12th and 13th century, and hence determine when forest dynamics started to be influenced by this invasive rodent species, but also to locate the forest edge at that time (**Fig. 6**). It is therefore possible to distinguish between the medieval forest and the modern one, providing an explanation for differences of soil and vegetation characteristics.

In sum, LiDAR data not only prompted an “archaeological revolution” by revealing unexpected past human activities and their intensity, but also play a crucial role to unravel the effects of these (pre)historical activities on current biodiversity and ecosystem functioning. More than ever, present ecosystems and landscapes must be viewed as a legacy of past interactions between humans and their environment.

Perspectives

Although we focused our review on the lagging dynamics of vegetation changes in the understory of European temperate forests, we suggest that the exact same suite of LiDAR-derived variables can also be used to study time-lag dynamics in the response of other taxonomic groups to macro-environmental changes. Indeed, plants in the understory layer provide food resources and microhabitats (i.e., microclimatic conditions) for other organisms living in, on, or near the soil surface. Therefore, time lags in vegetation changes can perpetuate and generate a domino effect on other taxa and interaction networks throughout complex aboveground-belowground linkages (Bardgett & Wardle, 2010). Such cascading effects not only involve bottom-up chain reactions across trophic levels (e.g., from primary producers to primary consumers or soil decomposers) (Valencia et al., 2018) but also top-down chain reactions. Indeed, changes in herbivore density or composition (e.g., ungulates or insects), sometimes driven by macroclimate warming and disrupted plant-herbivore interactions (Rasmann et al., 2014; Vitasse et al., 2021), can have long-term biological legacies on aboveground plant community composition (Hamann et al., 2021; Nuttle et al., 2014). For instance, Nuttle et al. (2014) showed that the initial density in white-tailed deer (*Odocoileus virginianus*) in Pennsylvania still influences current understory vegetation in 30-year-old, closed-canopy forests. In the meantime, LiDAR-derived variables have been successfully incorporated as predictor variables into models of species diversity and distribution across a wide range of taxonomic groups (de Vries et al., 2021; Farrell et al., 2013; Hattab et al., 2017; Moeslund et al., 2019; Simonson et al., 2014), often as a mean to capture local processes such as microclimates and biotic interactions (Lembrechts et al., 2019; Zellweger et al., 2019). Hence, LiDAR-derived variables have the potential to significantly improve species distribution modelling across a wide range of taxa, inform us on the structure of trophic webs, and therefore help us better understand time-lag dynamics perpetuating across trophic levels.

Remote sensing science continues to innovate and thus some research perspectives should be highlighted here. Innovations can come either from the LiDAR sensor itself, the combination with other sensors (e.g., coupling LiDAR data with hyperspectral images) or from other technologies. Typical LiDAR data retrieve discrete echoes in only one wavelength. Today, the two big new innovations in LiDAR technology are (1) the analysis on the full-waveform laser information and (2) the use of multispectral lasers, which bring both high resolution 3D point clouds and classical multispectral information. The first one allows much more precise information of surfaces than typical multi-echo LiDAR, especially for forest structure and composition (Fassnacht et al., 2016; Koenig & Höfle, 2016). The second allows the remote identification of tree species (Amiri et al., 2019) as well as the production of typical remote sensing indicators, such as normalized difference vegetation index (NDVI), for understory conditions not easily accessible with classical multispectral images that do not penetrate forest canopy cover. Additionally, data fusion remains one of the main interests in remote sensing technology. For example, hyperspectral data has proven its complementarity with LiDAR data to better understand ecosystem functioning (Ewald et al., 2018). While LiDAR data gives precise information about the 3D structure of surfaces, hyperspectral images give more precise information of surface reflectance (hundreds of spectral bands) than classical multispectral images. Hyperspectral data is thus more relevant than LiDAR data to provide information on stand composition and can help detect foliar traits and leaf chemical composition (Ewald et al., 2018). For instance, in terms of lagging dynamics involving past land uses, hyperspectral data could be used to locate particular pollutants in the upper canopy layer (for example perchlorates that affect photosynthesis and thus surface reflectance) as an indirect indicator of pollutant concentration in the soil (Wang et al., 2018) likely affecting plant species composition in the understory. Coupling LiDAR and hyperspectral data could therefore be of high interest and could give precious information of time-lag dynamics in biodiversity changes. Additionally, it is possible to combine LiDAR data from a single survey with other types of

technologies to monitor changes in forest structure over time and thus better understand time-lag dynamics in the forest understory. For example, photogrammetry can retrieve 3D surfaces to generate digital surface models (DSMs) at different time periods using time series of RGB images. Such time series of DSMs derived from photogrammetry could then be coupled with a single LiDAR-derived DTM to monitor changes in maximum canopy height over time (Michez et al., 2016). Pleiades satellites are interesting in this regard as they allow to produce DSMs across large spatial extents at a relatively low price. In line with Pleiades, the CO3D mission is a pioneer mission, planned to be launched by the CNES (the French Spatial Agency) in mid-2023. Ultimately, the CO3D mission will provide a worldwide high (1-m) resolution DSM in 2025. Combining past photogrammetric data sets, where available, with more recent time series of DSMs, from either airborne or spaceborne data, would also allow obtaining the longer-term data necessary to observe temporal dynamics.

Finally, there are exiting recent advances and open-source tools to overcome challenges associated with LiDAR data handling and processing (Atkins et al., 2022). First, recent packages developed for the R statistical software (R Core Team, 2021), such as the lidR (Roussel et al., 2020) and forestr package (Atkins et al., 2018) for ALS and TLS data, respectively, have greatly advanced the handling and processing of LiDAR data. Second, it is now possible to call programming languages such as Python, which is chiefly used by the remote sensing community, directly within the R environment, thanks to the reticulate package (Ushey et al., 2021). It is also possible and quite usual to wrap C/C++ functions within R. Using a compiled language allows a speedier execution when processing huge point cloud data sets. This, will allow ecologists – that are often most familiar with R – to better access the recent open-source tools developed and used by the remote sensing community. Third, recent advances in R and Python to use machine learning and deep learning algorithms (e.g., the keras Python library) (Kalinowski et al., 2021) will help to lift technical barriers in linking LiDAR data with ecological data from field observations. Finally, data

591 processing facilities continue to develop steadily, with increased access to data and computer

592 centres.

Conclusion

To conclude, LiDAR data can unveil past forest management interventions and even past land uses within temperate deciduous forests. LiDAR technology has the capacity to monitor and determine fine-grained structural information – namely: the vertical complexity of vegetation layering and the micro-topographic variations at the ground surface – invisible to the naked eye, providing far more information than conventional field surveys. Yet, LiDAR data alone is insufficient and still requires to be coupled with field surveys to calibrate models, validate predictions, and correct misclassifications of items. Besides, LiDAR technology needs a highly diverse set of expertise to unveil any useful information hidden in the data. Hence, LiDAR is a transdisciplinary tool for plant, soil, and historical ecologists as well as for foresters, archaeologists, and remote sensing scientists to work together and help each other advance their respective fields of research. With this in mind, we encourage plant and soil ecologists to work with historians, archaeologists, and remote sensing scientists in order to use meaningful LiDAR-derived variables, such as the ones we featured in this review (**Figs. 3-6**), as surrogates to capture time-lag dynamics in biotic responses to long-term macro-environmental changes. Doing so will ultimately help us better predict the current and future distribution of forest biodiversity.

"Inside every sane person there's a madman struggling to get out," said the shopkeeper. "That's what I've always thought. No one goes mad quicker than a totally sane person." –Terry Pratchett, The Light Fantastic (1986)

Acknowledgements

JL and EVG received funding from the Agence Nationale de la Recherche (ANR), under the framework of the young investigators (JCJC) funding instrument (ANR JCJC Grant project N°ANR-19-CE32-0005-01: IMPRINT). JL also acknowledges funding from the Centre National de la Recherche Scientifique (CNRS) (Défi INFINITI 2018: MORFO). CM and PDF received funding from the European Research Council (ERC) under the European Union's Horizon 2020 research and innovation programme (ERC Starting Grant FORMICA 757833). FZ received funding from the Swiss National Science Foundation (grant number 193645). DR was partially supported by the H2020 Project SHOWCASE (Grant agreement No 862480) and by the H2020 COST Action CA17134 'Optical synergies for spatiotemporal sensing of scalable ecophysiological traits' (SENSECO).

622 **Conflict of interest**

623 No conflict of interest to declare.

Authors' contributions

JL conceptualized the project, designed the review paper, wrote the introduction and conclusion sections, and led the writing. FZ and JJL co-led the writing of section 1 on using LiDAR to unveil past forest management practices with contributions from PDF, KVM, CM, RM, EVG, and DR. HH led the writing of section 2 on using LiDAR data to highlight soil compaction from skid trails with contributions from BB and GD. GD led the writing of section 3 on using LiDAR data to unveil past land uses with contributions from BB and JB. ML led the writing of section 4 on the perspectives with contribution from RM. SD, led the writing of Boxes 1 and 2 with contributions from SA and KD. EVG designed Fig. 1 with contribution from JL. SD designed Figs. 2 and 3 with contribution from JL. CM designed Fig. 4 with contribution from JL. EGM designed Fig. 5 with contribution from HH and JL. EGM & BB designed Fig.6 with contribution from JL. All authors significantly revised the manuscript and approved it for submission.

636 **Data availability**

637 No data was used in this essay review.

References

Alexander, J. M., Chalmandrier, L., Lenoir, J., Burgess, T. I., Essl, F., Haider, S., Kueffer, C., McDougall, K., Milbau, A., Nuñez, M. A., Pauchard, A., Rabitsch, W., Rew, L. J., Sanders, N. J., & Pellissier, L. (2018). Lags in the response of mountain plant communities to climate change. *Global Change Biology*, *24*(2), 563–579. https://doi.org/10.1111/gcb.13976

Almeida, D. R. A., Broadbent, E. N., Zambrano, A. M. A., Wilkinson, B. E., Ferreira, M. E., Chazdon, R., Meli, P., Gorgens, E. B., Silva, C. A., Stark, S. C., Valbuena, R., Papa, D. A., & Brancalion, P. H. S. (2019). Monitoring the structure of forest restoration plantations with a drone-lidar system. *International Journal of Applied Earth Observation and Geoinformation*, *79*, 192–198. https://doi.org/10.1016/j.jag.2019.03.014

Amiri, N., Krzystek, P., Heurich, M., & Skidmore, A. (2019). Classification of tree species as well as standing dead trees using triple wavelength ALS in a temperate forest. *Remote Sensing*, *11*(22), 2614. https://doi.org/10.3390/rs11222614

Arocena, J. M. (2000). Cations in solution from forest soils subjected to forest floor removal and compaction treatments. *Forest Ecology and Management*, *133*(1), 71–80. https://doi.org/10.1016/S0378-1127(99)00299-6

Atkins, J. W., Bohrer, G., Fahey, R. T., Hardiman, B. S., Morin, T. H., Stovall, A. E. L., Zimmerman, N., & Gough, C. M. (2018). Quantifying vegetation and canopy structural complexity from terrestrial LiDAR data using the forestr r package. *Methods in Ecology and Evolution*, *9*(10), 2057–2066. https://doi.org/10.1111/2041-210X.13061

Atkins, J. W., Stovall, A. E. L., & Alberto Silva, C. (2022). Open-Source tools in R for forestry and forest ecology. *Forest Ecology and Management*, *503*, 119813. https://doi.org/10.1016/j.foreco.2021.119813

Baeten, L., Bauwens, B., Schrijver, A. D., Keersmaeker, L. D., Calster, H. V., Vandekerkhove, K., Roelandt, B., Beeckman, H., & Verheyen, K. (2009). Herb layer changes (1954-2000) related to the conversion of coppice-with-standards forest and soil acidification. *Applied Vegetation Science*, *12*(2), 187–197. https://doi.org/10.1111/j.1654-109X.2009.01013.x

665 Bardgett, R. D., & Wardle, D. A. (2010). *Aboveground-belowground linkages: biotic interactions, ecosystem*
666 *processes, and global change*. Oxford University Press.
667 Bartha, S., Merolli, A., Campetella, G., & Canullo, R. (2008). Changes of vascular plant diversity along a
668 chronosequence of beech coppice stands, central Apennines, Italy. *Plant Biosystems - An*
669 *International Journal Dealing with All Aspects of Plant Biology*, *142*(3), 572–583.
670 https://doi.org/10.1080/11263500802410926
671 Becker, T., Spanka, J., Schröder, L., & Leuschner, C. (2017a). Forty years of vegetation change in former
672 coppice-with-standards woodlands as a result of management change and N deposition. *Applied*
673 *Vegetation Science*, *20*(2), 304–313. https://doi.org/10.1111/avsc.12282
674 Becker, T., Spanka, J., Schröder, L., & Leuschner, C. (2017b). Forty years of vegetation change in former
675 coppice-with-standards woodlands as a result of management change and N deposition. *Applied*
676 *Vegetation Science*, *20*(2), 304–313. https://doi.org/10.1111/avsc.12282
677 Bertrand, R., Lenoir, J., Piedallu, C., Riofrío-Dillon, G., de Ruffray, P., Vidal, C., Pierrat, J.-C., & Gégout, J.-C.
678 (2011). Changes in plant community composition lag behind climate warming in lowland forests.
679 *Nature*, *479*(7374), 517–520. https://doi.org/10.1038/nature10548
680 Bertrand, R., Riofrío-Dillon, G., Lenoir, J., Drapier, J., de Ruffray, P., Gégout, J.-C., & Loreau, M. (2016).
681 Ecological constraints increase the climatic debt in forests. *Nature Communications*, *7*, 12643.
682 https://doi.org/10.1038/ncomms12643
683 Bonhage, A., Hirsch, F., Schneider, A., Raab, A., Raab, T., & Donovan, S. (2020). Long term anthropogenic
684 enrichment of soil organic matter stocks in forest soils – Detecting a legacy of historical charcoal
685 production. *Forest Ecology and Management*, *459*, 117814.
686 https://doi.org/10.1016/j.foreco.2019.117814
687 Bottalico, F., Travaglini, D., Chirici, G., Marchetti, M., Marchi, E., Nocentini, S., & Corona, P. (2014).
688 Classifying silvicultural systems (coppices vs. high forests) in Mediterranean oak forests by Airborne
689 Laser Scanning data. *European Journal of Remote Sensing*, *47*(1), 437–460.
690 https://doi.org/10.5721/EuJRS20144725

691 Bouvier, M., Durrieu, S., Fournier, R. A., & Renaud, J.-P. (2015). Generalizing predictive models of forest
692 inventory attributes using an area-based approach with airborne LiDAR data. *Remote Sensing of*
693 *Environment*, *156*(Supplement C), 322–334. https://doi.org/10.1016/j.rse.2014.10.004
694 Brasseur, B., Spicher, F., Lenoir, J., Gallet-Moron, E., Buridant, J., & Horen, H. (2018). What deep-soil
695 profiles can teach us on deep-time pH dynamics after land use change? *Land Degradation &*
696 *Development*, *29*(9), 2951–2961. https://doi.org/10.1002/ldr.3065
697 Bricca, A., Chelli, S., Canullo, R., & Cutini, M. (2020). The legacy of the past logging: how forest structure
698 affects different facets of understory plant diversity in abandoned coppice forests. *Diversity*, *12*(3),
699 109. https://doi.org/10.3390/d12030109
700 Brice, M.-H., Cazelles, K., Legendre, P., & Fortin, M.-J. (2019). Disturbances amplify tree community
701 responses to climate change in the temperate–boreal ecotone. *Global Ecology and Biogeography*,
702 *28*(11), 1668–1681. https://doi.org/10.1111/geb.12971
703 Briggs, J. M., Spielmann, K. A., Schaafsma, H., Kintigh, K. W., Kruse, M., Morehouse, K., & Schollmeyer, K.
704 (2006). Why ecology needs archaeologists and archaeology needs ecologists. *Frontiers in Ecology*
705 *and the Environment*, *4*(4), 180–188. https://doi.org/10.1890/1540-
706 9295(2006)004[0180:WENAAA]2.0.CO;2
707 Buckley, D. S., Crow, T. R., Nauertz, E. A., & Schulz, K. E. (2003). Influence of skid trails and haul roads on
708 understory plant richness and composition in managed forest landscapes in Upper Michigan, USA.
709 *Forest Ecology and Management*, *175*(1), 509–520. https://doi.org/10.1016/S0378-1127(02)00185-
710 8
711 Bürgi, M., Östlund, L., & Mladenoff, D. J. (2017). Legacy effects of human land use: ecosystems as time-
712 lagged systems. *Ecosystems*, *20*(1), 94–103. https://doi.org/10.1007/s10021-016-0051-6
713 Cambi, M., Mariotti, B., Fabiano, F., Maltoni, A., Tani, A., Foderi, C., Laschi, A., & Marchi, E. (2018). Early
714 response of Quercus robur seedlings to soil compaction following germination. *Land Degradation &*
715 *Development*, *29*(4), 916–925. https://doi.org/10.1002/ldr.2912
716 Canuto, M. A., Estrada-Belli, F., Garrison, T. G., Houston, S. D., Acuña, M. J., Kováč, M., Marken, D.,
717 Nondédéo, P., Auld-Thomas, L., Castanet, C., Chatelain, D., Chiriboga, C. R., Drápela, T., Lieskovský,

718 T., Tokovinine, A., Velasquez, A., Fernández-Díaz, J. C., & Shrestha, R. (2018). Ancient lowland Maya
719 complexity as revealed by airborne laser scanning of northern Guatemala. *Science*, *361*(6409).
720 https://doi.org/10.1126/science.aau0137
721 Cauchemé, V. (1912). *Description des fouilles archéologiques exécutées dans la forêt de Compiègne.*
722 https://gallica.bnf.fr/ark:/12148/bpt6k5746626z
723 Chase, A. F., Chase, D. Z., Fisher, C. T., Leisz, S. J., & Weishampel, J. F. (2012). Geospatial revolution and
724 remote sensing LiDAR in Mesoamerican archaeology. *Proceedings of the National Academy of*
725 *Sciences*, *109*(32), 12916–12921. https://doi.org/10.1073/pnas.1205198109
726 Closset-Kopp, D., & Decocq, G. (2015). Remnant Artificial Habitats as Biodiversity Islets into Forest Oceans.
727 *Ecosystems*, *18*(3), 507–519. https://doi.org/10.1007/s10021-015-9843-3
728 Closset-Kopp, D., Hattab, T., & Decocq, G. (2019). Do drivers of forestry vehicles also drive herb layer
729 changes (1970–2015) in a temperate forest with contrasting habitat and management conditions?
730 *Journal of Ecology*, *107*(3), 1439–1456. https://doi.org/10.1111/1365-2745.13118
731 Costa, L., Laüt, L., & Petit, C. (2020). Archéologie, forêt et Lidar : une recherche qui a du relief !
732 Introduction. *Archéologies Numériques*, *1*(4), 1–7. https://doi.org/10.21494/ISTE.OP.2020.0536
733 Dambrine, E., Dupouey, J.-L., Laüt, L., Humbert, L., Thinon, M., Beaufils, T., & Richard, H. (2007). Present
734 forest biodiversity patterns in France related to former Roman agriculture. *Ecology*, *88*(6), 1430–
735 1439. https://doi.org/10.1890/05-1314
736 Dassot, M., Constant, T., & Fournier, M. (2011). The use of terrestrial LiDAR technology in forest science:
737 application fields, benefits and challenges. *Annals of Forest Science*, *68*(5), 959–974.
738 https://doi.org/10.1007/s13595-011-0102-2
739 De Frenne, P., Lenoir, J., Luoto, M., Scheffers, B. R., Zellweger, F., Aalto, J., Ashcroft, M. B., Christiansen, D.
740 M., Decocq, G., Pauw, K. D., Govaert, S., Greiser, C., Gril, E., Hampe, A., Jucker, T., Klinges, D. H.,
741 Koelemeijer, I. A., Lembrechts, J. J., Marrec, R., … Hylander, K. (2021). Forest microclimates and
742 climate change: Importance, drivers and future research agenda. *Global Change Biology*, *27*(11),
743 2279–2297. https://doi.org/10.1111/gcb.15569

De Frenne, P., Rodríguez-Sánchez, F., Coomes, D. A., Baeten, L., Verstraeten, G., Vellend, M., Bernhardt-Römermann, M., Brown, C. D., Brunet, J., Cornelis, J., Decocq, G. M., Dierschke, H., Eriksson, O., Gilliam, F. S., Hédl, R., Heinken, T., Hermy, M., Hommel, P., Jenkins, M. A., … Verheyen, K. (2013). Microclimate moderates plant responses to macroclimate warming. *Proceedings of the National Academy of Sciences*, *110*(46), 18561–18565. https://doi.org/10.1073/pnas.1311190110

De Lombaerde, E., Vangansbeke, P., Lenoir, J., Van Meerbeek, K., Lembrechts, J., Rodríguez-Sánchez, F., Luoto, M., Scheffers, B., Haesen, S., Aalto, J., Christiansen, D. M., De Pauw, K., Depauw, L., Govaert, S., Greiser, C., Hampe, A., Hylander, K., Klinges, D., Koelemeijer, I., … De Frenne, P. (2021). Maintaining forest cover to enhance temperature buffering under future climate change. *Science of The Total Environment*, 151338. https://doi.org/10.1016/j.scitotenv.2021.151338

De Schrijver, A., De Frenne, P., Staelens, J., Verstraeten, G., Muys, B., Vesterdal, L., Wuyts, K., van Nevel, L., Schelfhout, S., de Neve, S., & Verheyen, K. (2012). Tree species traits cause divergence in soil acidification during four decades of postagricultural forest development. *Global Change Biology*, *18*(3), 1127–1140. https://doi.org/10.1111/j.1365-2486.2011.02572.x

de Vries, J. P. R., Koma, Z., WallisDeVries, M. F., & Kissling, W. D. (2021). Identifying fine-scale habitat preferences of threatened butterflies using airborne laser scanning. *Diversity and Distributions*, *27*(7), 1251–1264. https://doi.org/10.1111/ddi.13272

Decocq, G., Aubert, M., Dupont, F., Alard, D., Saguez, R., Wattez-Franger, A., Foucault, B. D., Delelis-Dusollier, A., & Bardat, J. (2004). Plant diversity in a managed temperate deciduous forest: understorey response to two silvicultural systems. *Journal of Applied Ecology*, *41*(6), 1065–1079. https://doi.org/10.1111/j.0021-8901.2004.00960.x

Della Longa, G., Boscutti, F., Marini, L., & Alberti, G. (2020). Coppicing and plant diversity in a lowland wood remnant in North–East Italy. *Plant Biosystems - An International Journal Dealing with All Aspects of Plant Biology*, *154*(2), 173–180. https://doi.org/10.1080/11263504.2019.1578276

Desbordes, J.-M. (1973). La recherche archéologique sous-bois. *Revue archéologique de Picardie*, *3*(1), 12–12. https://doi.org/10.3406/pica.1973.1169

770 Devictor, V., van Swaay, C., Brereton, T., Brotons, L., Chamberlain, D., Heliölä, J., Herrando, S., Julliard, R.,
771 Kuussaari, M., Lindström, Å., Reif, J., Roy, D. B., Schweiger, O., Settele, J., Stefanescu, C., Van Strien,
772 A., Van Turnhout, C., Vermouzek, Z., WallisDeVries, M., … Jiguet, F. (2012). Differences in the
773 climatic debts of birds and butterflies at a continental scale. *Nature Climate Change*, *2*(2), 121–124.
774 https://doi.org/10.1038/nclimate1347
775 Dullinger, S., Gattringer, A., Thuiller, W., Moser, D., Zimmermann, N. E., Guisan, A., Willner, W., Plutzar, C.,
776 Leitner, M., Mang, T., Caccianiga, M., Dirnböck, T., Ertl, S., Fischer, A., Lenoir, J., Svenning, J.-C.,
777 Psomas, A., Schmatz, D. R., Silc, U., … Hülber, K. (2012). Extinction debt of high-mountain plants
778 under twenty-first-century climate change. *Nature Climate Change*, *2*(8), 619–622.
779 https://doi.org/10.1038/nclimate1514
780 Dupouey, J. L., Dambrine, E., Laffite, J. D., & Moares, C. (2002). Irreversible impact of past land use on forest
781 soils and biodiversity. *Ecology*, *83*(11), 2978–2984. https://doi.org/10.2307/3071833
782 Durrieu, S., Véga, C., Bouvier, M., Gosselin, F., Renaud, J. P., & Saint-André, L. (2015). Optical remote
783 sensing of tree and stand heights. In *Land Resources Monitoring, Modeling, and Mapping with*
784 *Remote Sensing* (1st Edition, pp. 449–485). CRC Press.
785 Ebeling, C., Lang, F., & Gaertig, T. (2016). Structural recovery in three selected forest soils after compaction
786 by forest machines in Lower Saxony, Germany. *Forest Ecology and Management*, *359*, 74–82.
787 https://doi.org/10.1016/j.foreco.2015.09.045
788 Etienne, D., Ruffaldi, P., Goepp, S., Ritz, F., Georges-Leroy, M., Pollier, B., & Dambrine, E. (2011). The origin
789 of closed depressions in Northeastern France: A new assessment. *Geomorphology*, *126*(1), 121–
790 131. https://doi.org/10.1016/j.geomorph.2010.10.036
791 Evans, D. H., Fletcher, R. J., Pottier, C., Chevance, J.-B., Soutif, D., Tan, B. S., Im, S., Ea, D., Tin, T., Kim, S.,
792 Cromarty, C., De Greef, S., Hanus, K., Bâty, P., Kuszinger, R., Shimoda, I., & Boornazian, G. (2013).
793 Uncovering archaeological landscapes at Angkor using lidar. *Proceedings of the National Academy*
794 *of Sciences*, *110*(31), 12595–12600.
795 Ewald, M., Aerts, R., Lenoir, J., Fassnacht, F. E., Nicolas, M., Skowronek, S., Piat, J., Honnay, O., Garzón-
796 López, C. X., Feilhauer, H., Van De Kerchove, R., Somers, B., Hattab, T., Rocchini, D., & Schmidtlein,

S. (2018). LiDAR derived forest structure data improves predictions of canopy N and P concentrations from imaging spectroscopy. *Remote Sensing of Environment*, *211*, 13–25. https://doi.org/10.1016/j.rse.2018.03.038

Farrell, S. L., Collier, B. A., Skow, K. L., Long, A. M., Campomizzi, A. J., Morrison, M. L., Hays, K. B., & Wilkins, R. N. (2013). Using LiDAR-derived vegetation metrics for high-resolution, species distribution models for conservation planning. *Ecosphere*, *4*(3), art42. https://doi.org/10.1890/ES12-000352.1

Fassnacht, F. E., Latifi, H., Stereńczak, K., Modzelewska, A., Lefsky, M., Waser, L. T., Straub, C., & Ghosh, A. (2016). Review of studies on tree species classification from remotely sensed data. *Remote Sensing of Environment*, *186*, 64–87. https://doi.org/10.1016/j.rse.2016.08.013

Forister, M. L., McCall, A. C., Sanders, N. J., Fordyce, J. A., Thorne, J. H., O'Brien, J., Waetjen, D. P., & Shapiro, A. M. (2010). Compounded effects of climate change and habitat alteration shift patterns of butterfly diversity. *Proceedings of the National Academy of Sciences*, *107*(5), 2088–2092. https://doi.org/10.1073/pnas.0909686107

Fouédjeu, L., Paradis-Grenouillet, S., Larrieu, L., Saulnier, M., Burri, S., & Py-Saragaglia, V. (2021). The socio-ecological legacies of centuries-old charcoal making practices in a mountain forest of the northern Pyrenees. *Forest Ecology and Management*, *502*, 119717. https://doi.org/10.1016/j.foreco.2021.119717

Frey, S. J. K., Hadley, A. S., Johnson, S. L., Schulze, M., Jones, J. A., & Betts, M. G. (2016). Spatial models reveal the microclimatic buffering capacity of old-growth forests. *Science Advances*, *2*(4), e1501392. https://doi.org/10.1126/sciadv.1501392

Fruchart, C. (2020). Le LiDAR : un outil pour l'étude archéologique des usages anciens des sols. *Archéologies Numériques*, *4*(1), 1–17. https://doi.org/10.21494/ISTE.OP.2020.0520

George, A. D., III, F. R. T., & Faaborg, J. (2015). Using LiDAR and remote microclimate loggers to downscale near-surface air temperatures for site-level studies. *Remote Sensing Letters*, *6*(12), 924–932. https://doi.org/10.1080/2150704X.2015.1088671

822 Georges-Leroy, M., Bock, J., Dambrine, É., & Dupouey, J.-L. (2011). Apport du lidar à la connaissance de
823 l'histoire de l'occupation du sol en forêt de Haye. *ArcheoSciences. Revue d'archéométrie*, *35*, 117–
824 129. https://doi.org/10.4000/archeosciences.3015
825 Germond, G., Champême, L.-M., & Fernandez, L. (1988). Le problème archéologique des Garennes.
826 *Archéologie Médiévale*, *18*(1), 239–254. https://doi.org/10.3406/arcme.1988.1211
827 Gilliam, F. S. (2007). The Ecological Significance of the Herbaceous Layer in Temperate Forest Ecosystems.
828 *BioScience*, *57*(10), 845–858. https://doi.org/10.1641/B571007
829 Godefroid, S., & Koedam, N. (2004). The impact of forest paths upon adjacent vegetation: effects of the
830 path surfacing material on the species composition and soil compaction. *Biological Conservation*,
831 *119*(3), 405–419. https://doi.org/10.1016/j.biocon.2004.01.003
832 Gottfried, M., Pauli, H., Futschik, A., Akhalkatsi, M., Barančok, P., Benito Alonso, J. L., Coldea, G., Dick, J.,
833 Erschbamer, B., Fernández Calzado, M. R., Kazakis, G., Krajči, J., Larsson, P., Mallaun, M., Michelsen,
834 O., Moiseev, D., Moiseev, P., Molau, U., Merzouki, A., … Grabherr, G. (2012). Continent-wide
835 response of mountain vegetation to climate change. *Nature Climate Change*, *2*(2), 111–115.
836 https://doi.org/10.1038/nclimate1329
837 Grotti, M., Calders, K., Origo, N., Puletti, N., Alivernini, A., Ferrara, C., & Chianucci, F. (2020). An intensity,
838 image-based method to estimate gap fraction, canopy openness and effective leaf area index from
839 phase-shift terrestrial laser scanning. *Agricultural and Forest Meteorology*, *280*, 107766.
840 https://doi.org/10.1016/j.agrformet.2019.107766
841 Guo, F., Lenoir, J., & Bonebrake, T. C. (2018). Land-use change interacts with climate to determine
842 elevational species redistribution. *Nature Communications*, *9*(1), 1315.
843 https://doi.org/10.1038/s41467-018-03786-9
844 Hamann, E., Blevins, C., Franks, S. J., Jameel, M. I., & Anderson, J. T. (2021). Climate change alters plant–
845 herbivore interactions. *New Phytologist*, *229*(4), 1894–1910. https://doi.org/10.1111/nph.17036
846 Hattab, T., Garzón-López, C. X., Ewald, M., Skowronek, S., Aerts, R., Horen, H., Brasseur, B., Gallet-Moron,
847 E., Spicher, F., Decocq, G., Feilhauer, H., Honnay, O., Kempeneers, P., Schmidtlein, S., Somers, B.,
848 Van De Kerchove, R., Rocchini, D., & Lenoir, J. (2017). A unified framework to model the potential

and realized distributions of invasive species within the invaded range. *Diversity and Distributions*, *23*(7), 806–819. https://doi.org/10.1111/ddi.12566

Hermy, M., Honnay, O., Firbank, L., Grashof-Bokdam, C., & Lawesson, J. E. (1999). An ecological comparison between ancient and other forest plant species of Europe, and the implications for forest conservation. *Biological Conservation*, *91*(1), 9–22. https://doi.org/10.1016/S0006-3207(99)00045-2

Hesse, R. (2010). LiDAR-derived Local Relief Models – a new tool for archaeological prospection. *Archaeological Prospection*, *17*(2), 67–72. https://doi.org/10.1002/arp.374

Inomata, T., Triadan, D., Vázquez López, V. A., Fernandez-Diaz, J. C., Omori, T., Méndez Bauer, M. B., García Hernández, M., Beach, T., Cagnato, C., Aoyama, K., & Nasu, H. (2020). Monumental architecture at Aguada Fénix and the rise of Maya civilization. *Nature*, *582*(7813), 530–533. https://doi.org/10.1038/s41586-020-2343-4

Jung, M., Rowhani, P., & Scharlemann, J. P. W. (2019). Impacts of past abrupt land change on local biodiversity globally. *Nature Communications*, *10*(1), 5474. https://doi.org/10.1038/s41467-019-13452-3

Kalinowski, T., Falbel, D., Allaire, J. J., Chollet, F., RStudio, Google, Tang [ctb, Y., cph, Bijl, W. V. D., Studer, M., & Keydana, S. (2021). *keras: R Interface to "Keras"* (Version 2.7.0) [Computer software]. https://CRAN.R-project.org/package=keras

Karlsson, J., Segerström, U., Berg, A., Mattielli, N., & Bindler, R. (2015). Tracing modern environmental conditions to their roots in early mining, metallurgy, and settlement in Gladhammar, southeast Sweden: Vegetation and pollution history outside the traditional Bergslagen mining region. *The Holocene*, *25*(6), 944–955. https://doi.org/10.1177/0959683615574586

Kharouba, H. M., Ehrlén, J., Gelman, A., Bolmgren, K., Allen, J. M., Travers, S. E., & Wolkovich, E. M. (2018). Global shifts in the phenological synchrony of species interactions over recent decades. *Proceedings of the National Academy of Sciences*, *115*(20), 5211–5216.

Knox, R. G., Peet, R. K., & Christensen, N. L. (1989). Population Dynamics in Loblolly Pine Stands: Changes in Skewness and Size Inequality. *Ecology*, *70*(4), 1153–1166. https://doi.org/10.2307/1941383

Koenig, K., & Höfle, B. (2016). Full-waveform airborne laser scanning in vegetation studies — a review of point cloud and waveform features for tree species classification. *Forests*, *7*(9), 198. https://doi.org/10.3390/f7090198

Koren, M., Slančík, M., Suchomel, J., & Dubina, J. (2015). Use of terrestrial laser scanning to evaluate the spatial distribution of soil disturbance by skidding operations. *IForest - Biogeosciences and Forestry*, *8*(3), 386. https://doi.org/10.3832/ifor1165-007

Kozlowski, T. T. (1999). Soil compaction and growth of woody plants. *Scandinavian Journal of Forest Research*, *14*(6), 596–619. https://doi.org/10.1080/02827589908540825

Laffite, J., Dambrine, É., Dupouey, J., & Georges-Leroy, M. (2002). Le parcellaire gallo-romain de la forêt domaniale de Saint-Amond à Favières (Meurthe-et-Moselle) : Relevé et étude du parcellaire du « Grand Rinchard ». *Revue Archéologique de l'Est*, *51*, 465–476.

Landuyt, D., Lombaerde, E. D., Perring, M. P., Hertzog, L. R., Ampoorter, E., Maes, S. L., Frenne, P. D., Ma, S., Proesmans, W., Blondeel, H., Sercu, B. K., Wang, B., Wasof, S., & Verheyen, K. (2019). The functional role of temperate forest understorey vegetation in a changing world. *Global Change Biology*, *25*(11), 3625–3641. https://doi.org/10.1111/gcb.14756

Larsen, T. H. (2012). Upslope range shifts of Andean dung beetles in response to deforestation: compounding and confounding effects of microclimatic change. *Biotropica*, *44*(1), 82–89. https://doi.org/10.1111/j.1744-7429.2011.00768.x

Lembrechts, J. J., Nijs, I., & Lenoir, J. (2019). Incorporating microclimate into species distribution models. *Ecography*, *42*(7), 1267–1279. https://doi.org/10.1111/ecog.03947

Lenoir, J., Bertrand, R., Comte, L., Bourgeaud, L., Hattab, T., Murienne, J., & Grenouillet, G. (2020). Species better track climate warming in the oceans than on land. *Nature Ecology & Evolution*, *4*(8), 1044–1059. https://doi.org/10.1038/s41559-020-1198-2

Lenoir, J., Decocq, G., Spicher, F., Gallet-Moron, E., Buridant, J., & Closset-Kopp, D. (2021). Historical continuity and spatial connectivity ensure hedgerows are effective corridors for forest plants: Evidence from the species–time–area relationship. *Journal of Vegetation Science*, *32*(1), e12845. https://doi.org/10.1111/jvs.12845

Lenoir, J., Hattab, T., & Pierre, G. (2017). Climatic microrefugia under anthropogenic climate change: implications for species redistribution. *Ecography*, *40*(2), 253–266. https://doi.org/10.1111/ecog.02788

Lindborg, R., & Eriksson, O. (2004). Historical landscape connectivity affects present plant species diversity. *Ecology*, *85*(7), 1840–1845.

Marra, E., Cambi, M., Fernandez-Lacruz, R., Giannetti, F., Marchi, E., & Nordfjell, T. (2018). Photogrammetric estimation of wheel rut dimensions and soil compaction after increasing numbers of forwarder passes. *Scandinavian Journal of Forest Research*, *33*(6), 613–620. https://doi.org/10.1080/02827581.2018.1427789

Maury, A. (1850). *Histoire des grandes forêts de la Gaule et de l'ancienne France*. https://gallica.bnf.fr/ark:/12148/bpt6k695760

Metzger, J. P., Martensen, A. C., Dixo, M., Bernacci, L. C., Ribeiro, M. C., Teixeira, A. M. G., & Pardini, R. (2009). Time-lag in biological responses to landscape changes in a highly dynamic Atlantic forest region. *Biological Conservation*, *142*(6), 1166–1177. https://doi.org/10.1016/j.biocon.2009.01.033

Meylemans, E., De Bie, M., Creemers, G., & Paesen, J. (2015). Revealing extensive protohistoric field systems through high resolution lidar data in the northern part of Belgium. *Archäeologisches Korrespondenzblatt*. https://www.academia.edu/37167453/Revealing_extensive_protohistoric_field_systems_through_high_resolution_lidar_data_in_the_northern_part_of_Belgium

Michez, A., Piégay, H., Lisein, J., Claessens, H., & Lejeune, P. (2016). Classification of riparian forest species and health condition using multi-temporal and hyperspatial imagery from unmanned aerial system. *Environmental Monitoring and Assessment*, *188*(3), 146. https://doi.org/10.1007/s10661-015-4996-2

Moeslund, J. E., Zlinszky, A., Ejrnæs, R., Brunbjerg, A. K., Bøcher, P. K., Svenning, J.-C., & Normand, S. (2019). Light detection and ranging explains diversity of plants, fungi, lichens, and bryophytes across multiple habitats and large geographic extent. *Ecological Applications*, *29*(5), e01907. https://doi.org/10.1002/eap.1907

Mohieddinne, H., Brasseur, B., Spicher, F., Gallet-Moron, E., Buridant, J., Kobaissi, A., & Horen, H. (2019). Physical recovery of forest soil after compaction by heavy machines, revealed by penetration resistance over multiple decades. *Forest Ecology and Management*, *449*, 117472. https://doi.org/10.1016/j.foreco.2019.117472

Moore, J.-D., & Ouimet, R. (2021). Liming still positively influences sugar maple nutrition, vigor and growth, 20 years after a single application. *Forest Ecology and Management*, *490*, 119103. https://doi.org/10.1016/j.foreco.2021.119103

Müllerová, J., Hédl, R., & Szabó, P. (2015). Coppice abandonment and its implications for species diversity in forest vegetation. *Forest Ecology and Management*, *343*, 88–100. https://doi.org/10.1016/j.foreco.2015.02.003

Neukom, R., Steiger, N., Gómez-Navarro, J. J., Wang, J., & Werner, J. P. (2019). No evidence for globally coherent warm and cold periods over the preindustrial Common Era. *Nature*, *571*(7766), 550–554. https://doi.org/10.1038/s41586-019-1401-2

Niemi, M. T., Vastaranta, M., Vauhkonen, J., Melkas, T., & Holopainen, M. (2017). Airborne LiDAR-derived elevation data in terrain trafficability mapping. *Scandinavian Journal of Forest Research*, *32*(8), 762–773. https://doi.org/10.1080/02827581.2017.1296181

Nuttle, T., Ristau, T. E., & Royo, A. A. (2014). Long-term biological legacies of herbivore density in a landscape-scale experiment: forest understoreys reflect past deer density treatments for at least 20 years. *Journal of Ecology*, *102*(1), 221–228. https://doi.org/10.1111/1365-2745.12175

Oettel, J., & Lapin, K. (2021). Linking forest management and biodiversity indicators to strengthen sustainable forest management in Europe. *Ecological Indicators*, *122*, 107275. https://doi.org/10.1016/j.ecolind.2020.107275

Oliveira, C., Aravecchia, S., Pradalier, C., Robin, V., & Devin, S. (2021). The use of remote sensing tools for accurate charcoal kilns' inventory and distribution analysis: Comparative assessment and prospective. *International Journal of Applied Earth Observation and Geoinformation*, *105*, 102641. https://doi.org/10.1016/j.jag.2021.102641

Panetta, A. M., Stanton, M. L., & Harte, J. (2018). Climate warming drives local extinction: Evidence from observation and experimentation. *Science Advances*, *4*(2), eaaq1819. https://doi.org/10.1126/sciadv.aaq1819

Perring, M. P., Bernhardt-Römermann, M., Baeten, L., Midolo, G., Blondeel, H., Depauw, L., Landuyt, D., Maes, S. L., Lombaerde, E. D., Carón, M. M., Vellend, M., Brunet, J., Chudomelová, M., Decocq, G., Diekmann, M., Dirnböck, T., Dörfler, I., Durak, T., Frenne, P. D., … Verheyen, K. (2018). Global environmental change effects on plant community composition trajectories depend upon management legacies. *Global Change Biology*, *24*(4), 1722–1740. https://doi.org/10.1111/gcb.14030

Peterken, G. F., & Game, M. (1984). Historical factors affecting the number and distribution of vascular plant species in the woodlands of central Lincolnshire. *Journal of Ecology*, *72*(1), 155–182. https://doi.org/10.2307/2260011

Plue, J., Hermy, M., Verheyen, K., Thuillier, P., Saguez, R., & Decocq, G. (2008). Persistent changes in forest vegetation and seed bank 1,600 years after human occupation. *Landscape Ecology*, *23*(6), 673–688. https://doi.org/10.1007/s10980-008-9229-4

Plue, J., Meuris, S., Verheyen, K., & Hermy, M. (2009). The importance of artefacts of ancient land use on plant communities in Meerdaal forest, Belgium. *Belgian Journal of Botany*, *142*(1), 3–18.

R Core Team. (2021). *R: A Language and Environment for Statistical Computing*. https://www.R-project.org/

Rackham, O. (2008). Ancient woodlands: modern threats. *New Phytologist*, *180*(3), 571–586. https://doi.org/10.1111/j.1469-8137.2008.02579.x

Rasmann, S., Pellissier, L., Defossez, E., Jactel, H., & Kunstler, G. (2014). Climate-driven change in plant–insect interactions along elevation gradients. *Functional Ecology*, *28*(1), 46–54. https://doi.org/10.1111/1365-2435.12135

Rassat, S., & Hugonnier, L. (2017). Atteindre l'histoire de la forêt de Compiègne par la télédétection aérienne et l'exploration des archives du sol. *Histoire & Mesure*, *XXXII*(XXXII–2), 67–102. https://doi.org/10.4000/histoiremesure.6136

Ren, S., He, K., Girshick, R., & Sun, J. (2017). Faster R-CNN: Towards Real-Time Object Detection with region proposal networks. *IEEE Transactions on Pattern Analysis and Machine Intelligence*, *39*(06), 1137–1149. https://doi.org/10.1109/TPAMI.2016.2577031

Richard, B., Dupouey, J.-L., Corcket, E., Alard, D., Archaux, F., Aubert, M., Boulanger, V., Gillet, F., Langlois, E., Macé, S., Montpied, P., Beaufils, T., Begeot, C., Behr, P., Boissier, J.-M., Camaret, S., Chevalier, R., Decocq, G., Dumas, Y., … Lenoir, J. (2021). The climatic debt is growing in the understorey of temperate forests: Stand characteristics matter. *Global Ecology and Biogeography*, *n/a*(n/a). https://doi.org/10.1111/geb.13312

Riofrío-Dillon, G., Bertrand, R., & Gégout, J.-C. (2012). Toward a recovery time: forest herbs insight related to anthropogenic acidification. *Global Change Biology*, *18*(11), 3383–3394. https://doi.org/10.1111/gcb.12002

Roussel, J.-R., Auty, D., Coops, N. C., Tompalski, P., Goodbody, T. R. H., Meador, A. S., Bourdon, J.-F., de Boissieu, F., & Achim, A. (2020). lidR: An R package for analysis of Airborne Laser Scanning (ALS) data. *Remote Sensing of Environment*, *251*, 112061. https://doi.org/10.1016/j.rse.2020.112061

Rumpf, S. B., Hülber, K., Wessely, J., Willner, W., Moser, D., Gattringer, A., Klonner, G., Zimmermann, N. E., & Dullinger, S. (2019). Extinction debts and colonization credits of non-forest plants in the European Alps. *Nature Communications*, *10*(1), 4293. https://doi.org/10.1038/s41467-019-12343-x

Rutkiewicz, P., Malik, I., Wistuba, M., & Osika, A. (2019). High concentration of charcoal hearth remains as legacy of historical ferrous metallurgy in southern Poland. *Quaternary International*, *512*, 133–143. https://doi.org/10.1016/j.quaint.2019.04.015

Schmitz, A., Sanders, T. G. M., Bolte, A., Bussotti, F., Dirnböck, T., Johnson, J., Peñuelas, J., Pollastrini, M., Prescher, A.-K., Sardans, J., Verstraeten, A., & de Vries, W. (2019). Responses of forest ecosystems in Europe to decreasing nitrogen deposition. *Environmental Pollution*, *244*, 980–994. https://doi.org/10.1016/j.envpol.2018.09.101

Simonson, W. D., Allen, H. D., & Coomes, D. A. (2014). Applications of airborne lidar for the assessment of animal species diversity. *Methods in Ecology and Evolution*, *5*(8), 719–729. https://doi.org/10.1111/2041-210X.12219

1009 Soma, M., Pimont, F., Durrieu, S., & Dupuy, J.-L. (2018). Enhanced measurements of leaf area density with
1010 T-LiDAR: Evaluating and calibrating the effects of vegetation heterogeneity and scanner properties.
1011 *Remote Sensing*, *10*(10), 1580. https://doi.org/10.3390/rs10101580
1012 Staude, I. R., Waller, D. M., Bernhardt-Römermann, M., Bjorkman, A. D., Brunet, J., De Frenne, P., Hédl, R.,
1013 Jandt, U., Lenoir, J., Máliš, F., Verheyen, K., Wulf, M., Pereira, H. M., Vangansbeke, P., Ortmann-
1014 Ajkai, A., Pielech, R., Berki, I., Chudomelová, M., Decocq, G., … Baeten, L. (2020). Replacements of
1015 small- by large-ranged species scale up to diversity loss in Europe's temperate forest biome. *Nature*
1016 *Ecology & Evolution*, *4*(6), 802–808. https://doi.org/10.1038/s41559-020-1176-8
1017 Stereńczak, K., Zapłata, R., Wójcik, J., Kraszewski, B., Mielcarek, M., Mitelsztedt, K., Białczak, M., Krok, G.,
1018 Kuberski, Ł., Markiewicz, A., Modzelewska, A., Parkitna, K., Piasecka, Ż., Pilch, K., Rzeczycki, K.,
1019 Sadkowski, R., Wietecha, M., Rysiak, P., von Gadow, K., & Cieszewski, C. J. (2020). ALS-based
1020 detection of past human activities in the Białowieża forest — new evidence of unknown remains of
1021 past agricultural systems. *Remote Sensing*, *12*(16), 2657. https://doi.org/10.3390/rs12162657
1022 Stickley, S. F., & Fraterrigo, J. M. (2021). Understory vegetation contributes to microclimatic buffering of
1023 near-surface temperatures in temperate deciduous forests. *Landscape Ecology*, *36*(4), 1197–1213.
1024 https://doi.org/10.1007/s10980-021-01195-w
1025 Storkey, J., Macdonald, A. J., Poulton, P. R., Scott, T., Köhler, I. H., Schnyder, H., Goulding, K. W. T., &
1026 Crawley, M. J. (2015). Grassland biodiversity bounces back from long-term nitrogen addition.
1027 *Nature*, *528*(7582), 401–404. https://doi.org/10.1038/nature16444
1028 Štular, B., Lozić, E., & Eichert, S. (2021). Airborne LiDAR-derived digital elevation model for archaeology.
1029 *Remote Sensing*, *13*(9), 1855. https://doi.org/10.3390/rs13091855
1030 Svenning, J.-C., & Sandel, B. (2013). Disequilibrium vegetation dynamics under future climate change.
1031 *American Journal of Botany*, *100*(7), 1266–1286. https://doi.org/10.3732/ajb.1200469
1032 Szabó, P. (2015). Historical ecology: past, present and future. *Biological Reviews*, *90*(4), 997–1014.
1033 https://doi.org/10.1111/brv.12141

1034 Talbot, B., Rahlf, J., & Astrup, R. (2018). An operational UAV-based approach for stand-level assessment of
1035 soil disturbance after forest harvesting. *Scandinavian Journal of Forest Research*, *33*(4), 387–396.
1036 https://doi.org/10.1080/02827581.2017.1418421
1037 Tan, K., Zhang, W., Shen, F., & Cheng, X. (2018). Investigation of TLS Intensity Data and Distance
1038 Measurement Errors from Target Specular Reflections. *Remote Sensing*, *10*(7), 1077.
1039 https://doi.org/10.3390/rs10071077
1040 Trier, Ø. D., Reksten, J. H., & Løseth, K. (2021). Automated mapping of cultural heritage in Norway from
1041 airborne lidar data using faster R-CNN. *International Journal of Applied Earth Observation and*
1042 *Geoinformation*, *95*, 102241. https://doi.org/10.1016/j.jag.2020.102241
1043 Ushey, K., Allaire, J. J., Tang, Y., Eddelbuettel, D., Lewis, B., Keydana, S., Hafen, R., & Geelnard, M. (2021).
1044 *reticulate: Interface to "Python" version 1.22 from CRAN* (Version 1.22) [Computer software].
1045 https://CRAN.R-project.org/package=reticulate. https://github.com/rstudio/reticulate
1046 Valbuena, R., Eerikäinen, K., Packalen, P., & Maltamo, M. (2016). Gini coefficient predictions from airborne
1047 lidar remote sensing display the effect of management intensity on forest structure. *Ecological*
1048 *Indicators*, *60*, 574–585. https://doi.org/10.1016/j.ecolind.2015.08.001
1049 Valdés, A., Lenoir, J., Gallet-Moron, E., Andrieu, E., Brunet, J., Chabrerie, O., Closset-Kopp, D., Cousins, S. A.
1050 O., Deconchat, M., Frenne, P. D., Smedt, P. D., Diekmann, M., Hansen, K., Hermy, M., Kolb, A., Liira,
1051 J., Lindgren, J., Naaf, T., Paal, T., … Decocq, G. (2015). The contribution of patch-scale conditions is
1052 greater than that of macroclimate in explaining local plant diversity in fragmented forests across
1053 Europe. *Global Ecology and Biogeography*, *24*(9), 1094–1105. https://doi.org/10.1111/geb.12345
1054 Valencia, E., Gross, N., Quero, J. L., Carmona, C. P., Ochoa, V., Gozalo, B., Delgado-Baquerizo, M., Dumack,
1055 K., Hamonts, K., Singh, B. K., Bonkowski, M., & Maestre, F. T. (2018). Cascading effects from plants
1056 to soil microorganisms explain how plant species richness and simulated climate change affect soil
1057 multifunctionality. *Global Change Biology*, *24*(12), 5642–5654. https://doi.org/10.1111/gcb.14440
1058 van Dobben, H. F., & de Vries, W. (2017). The contribution of nitrogen deposition to the eutrophication
1059 signal in understorey plant communities of European forests. *Ecology and Evolution*, *7*(1), 214–227.
1060 https://doi.org/10.1002/ece3.2485

1061 Vanwalleghem, T., Verheyen, K., Hermy, M., Poesen, J., & Deckers, J. (2004). Legacies of Roman land-use in
1062 the present-day vegetation in Meerdaal Forest (Belgium)? *Belgian Journal of Botany*, *137*(2), 181–
1063 187.
1064 Venier, L. A., Swystun, T., Mazerolle, M. J., Kreutzweiser, D. P., Wainio-Keizer, K. L., McIlwrick, K. A., Woods,
1065 M. E., & Wang, X. (2019). Modelling vegetation understory cover using LiDAR metrics. *PLOS ONE*,
1066 *14*(11), e0220096. https://doi.org/10.1371/journal.pone.0220096
1067 Verheyen, K., Bossuyt, B., Honnay, O., & Hermy, M. (2003). Herbaceous plant community structure of
1068 ancient and recent forests in two contrasting forest types. *Basic and Applied Ecology*, *4*(6), 537–
1069 546. https://doi.org/10.1078/1439-1791-00210
1070 Vincent, G., Antin, C., Laurans, M., Heurtebize, J., Durrieu, S., Lavalley, C., & Dauzat, J. (2017). Mapping
1071 plant area index of tropical evergreen forest by airborne laser scanning. A cross-validation study
1072 using LAI2200 optical sensor. *Remote Sensing of Environment*, *198*, 254–266.
1073 https://doi.org/10.1016/j.rse.2017.05.034
1074 Vitasse, Y., Ursenbacher, S., Klein, G., Bohnenstengel, T., Chittaro, Y., Delestrade, A., Monnerat, C., Rebetez,
1075 M., Rixen, C., Strebel, N., Schmidt, B. R., Wipf, S., Wohlgemuth, T., Yoccoz, N. G., & Lenoir, J. (2021).
1076 Phenological and elevational shifts of plants, animals and fungi under climate change in the
1077 European Alps. *Biological Reviews*, *n/a*(n/a). https://doi.org/10.1111/brv.12727
1078 Walter, J. A., Stovall, A. E. L., & Atkins, J. W. (2021). Vegetation structural complexity and biodiversity in the
1079 Great Smoky Mountains. *Ecosphere*, *12*(3), e03390. https://doi.org/10.1002/ecs2.3390
1080 Wang, F., Gao, J., & Zha, Y. (2018). Hyperspectral sensing of heavy metals in soil and vegetation: Feasibility
1081 and challenges. *ISPRS Journal of Photogrammetry and Remote Sensing*, *136*, 73–84.
1082 https://doi.org/10.1016/j.isprsjprs.2017.12.003
1083 Warren, M. S., Hill, J. K., Thomas, J. A., Asher, J., Fox, R., Huntley, B., Roy, D. B., Telfer, M. G., Jeffcoate, S.,
1084 Harding, P., Jeffcoate, G., Willis, S. G., Greatorex-Davies, J. N., Moss, D., & Thomas, C. D. (2001).
1085 Rapid responses of British butterflies to opposing forces of climate and habitat change. *Nature*,
1086 *414*(6859), 65. https://doi.org/10.1038/35102054

1087 Wei, L., Archaux, F., Hulin, F., Bilger, I., & Gosselin, F. (2020). Stand attributes or soil micro-environment
1088 exert greater influence than management type on understory plant diversity in even-aged oak high
1089 forests. *Forest Ecology and Management*, *460*, 117897.
1090 https://doi.org/10.1016/j.foreco.2020.117897
1091 Wei, L., Villemey, A., Hulin, F., Bilger, I., Yann, D., Chevalier, R., Archaux, F., & Gosselin, F. (2015). Plant
1092 diversity on skid trails in oak high forests: A matter of disturbance, micro-environmental conditions
1093 or forest age? *Forest Ecology and Management*, *338*, 20–31.
1094 https://doi.org/10.1016/j.foreco.2014.11.018
1095 White, J. C., Coops, N. C., Wulder, M. A., Vastaranta, M., Hilker, T., & Tompalski, P. (2016). Remote sensing
1096 technologies for enhancing forest inventories: a review. *Canadian Journal of Remote Sensing*, *42*(5),
1097 619–641. https://doi.org/10.1080/07038992.2016.1207484
1098 Williamson, T. (2008). *The archaeology of rabbit warrens*. Bloomsbury USA.
1099 Wulder, M. A., Coops, N. C., Hudak, A. T., Morsdorf, F., Nelson, R., Newnham, G., & Vastaranta, M. (2013).
1100 Status and prospects for LiDAR remote sensing of forested ecosystems. *Canadian Journal of Remote*
1101 *Sensing*, *39*(sup1), S1–S5. https://doi.org/10.5589/m13-051
1102 Zadora-Rio, E. (1986). Parcs à gibier et garennes à lapins : contribution à une étude archéologique des
1103 territoires de chasse dans le paysage médiéval. *Hommes et Terres du Nord*, *2*(1), 133–139.
1104 https://doi.org/10.3406/htn.1986.2054
1105 Zellweger, F., De Frenne, P., Lenoir, J., Rocchini, D., & Coomes, D. (2019). Advances in microclimate ecology
1106 arising from remote sensing. *Trends in Ecology & Evolution*, *34*(4), 327–341.
1107 https://doi.org/10.1016/j.tree.2018.12.012
1108 Zellweger, F., Frenne, P. D., Lenoir, J., Vangansbeke, P., Verheyen, K., Bernhardt-Römermann, M., Baeten,
1109 L., Hédl, R., Berki, I., Brunet, J., Calster, H. V., Chudomelová, M., Decocq, G., Dirnböck, T., Durak, T.,
1110 Heinken, T., Jaroszewicz, B., Kopecký, M., Máliš, F., … Coomes, D. (2020). Forest microclimate
1111 dynamics drive plant responses to warming. *Science*, *368*(6492), 772–775.
1112 https://doi.org/10.1126/science.aba6880

1113 Zhang, Z., Lv, Y., & Pan, H. (2013). Cooling and humidifying effect of plant communities in subtropical urban
1114 parks. *Urban Forestry & Urban Greening*, *12*(3), 323–329.
1115 https://doi.org/10.1016/j.ufug.2013.03.010
1116

1117 **Figure 1**

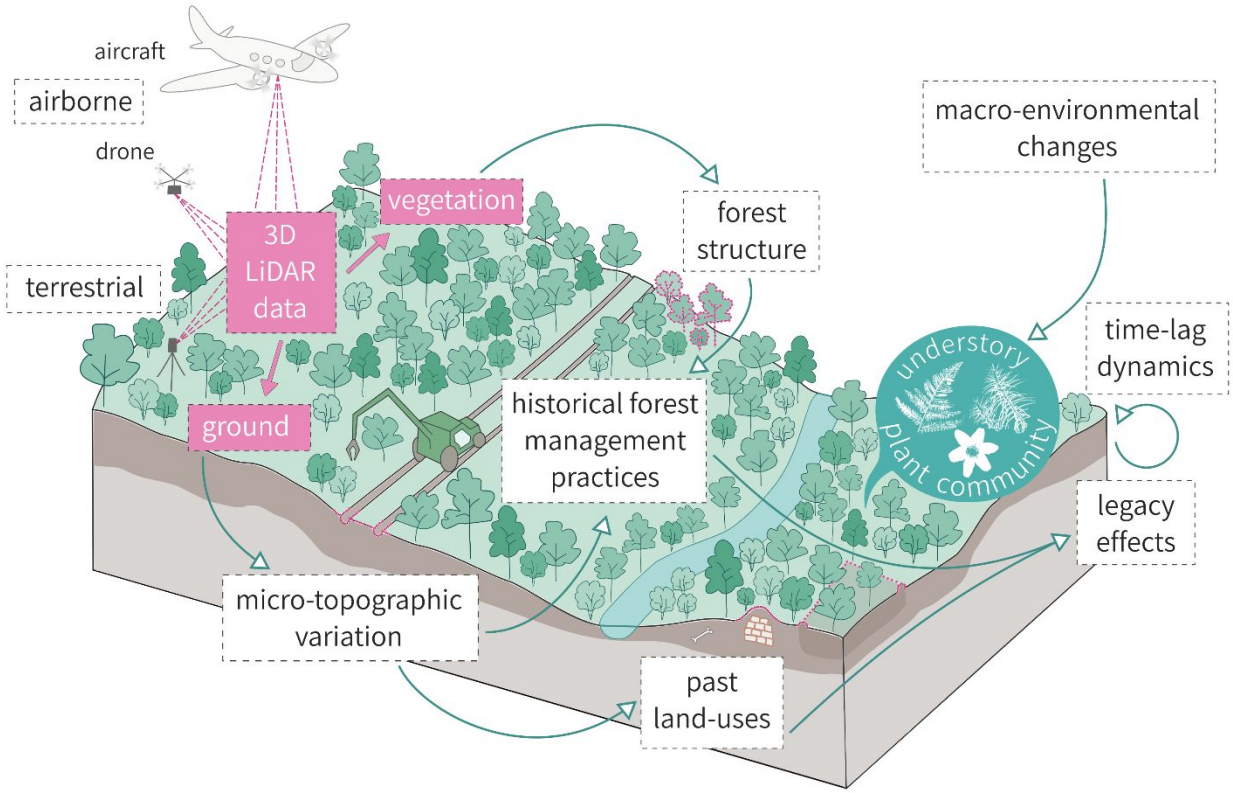

1118 **Fig. 1:** Conceptual figure illustrating how light detection and ranging (LiDAR) data can be used to
1119 assess micro-topographic variation (e.g., skid trails) and forest structure (e.g., vertical layering of
1120 vegetation) at a landscape level, and thus highlight legacy effects still affecting the current
1121 composition of understory plant communities and their responses to macro-environmental
1122 changes through time-lag dynamics. For instance, using well-chosen LiDAR-derived variables (see
1123 the main text and subsequent figures), it is possible to not only capture the imprints of historical
1124 forest management practices (e.g., ancient coppice-with-standards converted to high forests after
1125 World War II or the more recent intensification of heavy vehicles' traffic to harvest timber) but
1126 also to unveil past land uses (e.g., ancient settlements or agricultural fields).

1127 **Figure 2**

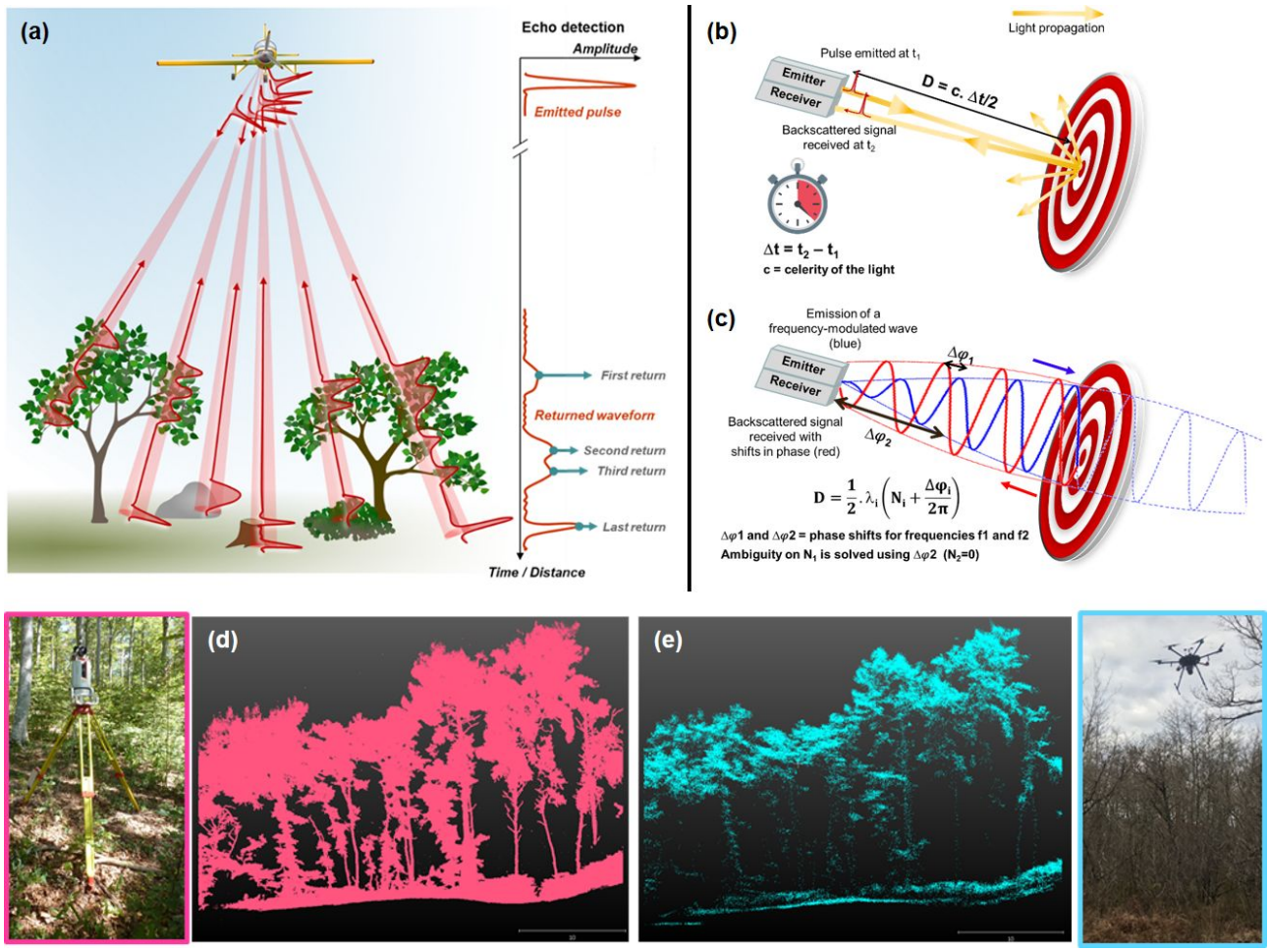

1128 **Fig. 2:** How light detection and ranging (LiDAR) works (a, b, c) and the mean to acquire LiDAR data
1129 from below or from above treetops (d, e). Upper-left panel (a): example of a non-stationary
1130 airborne LiDAR system (ALS) on board an aircraft. Upper-right panels (b, c): basic principles of
1131 time-of-flight vs. phase-shift LiDAR. Lower panels (d, e): data visualization of raw LiDAR point
1132 clouds extracted from both a stationary terrestrial LiDAR system (TLS) (Riegl VZ400) and a non-
1133 stationary ALS (YellowScan Vx20) covering the exact same study area in the Aigoual forest
1134 (France).

Figure 3

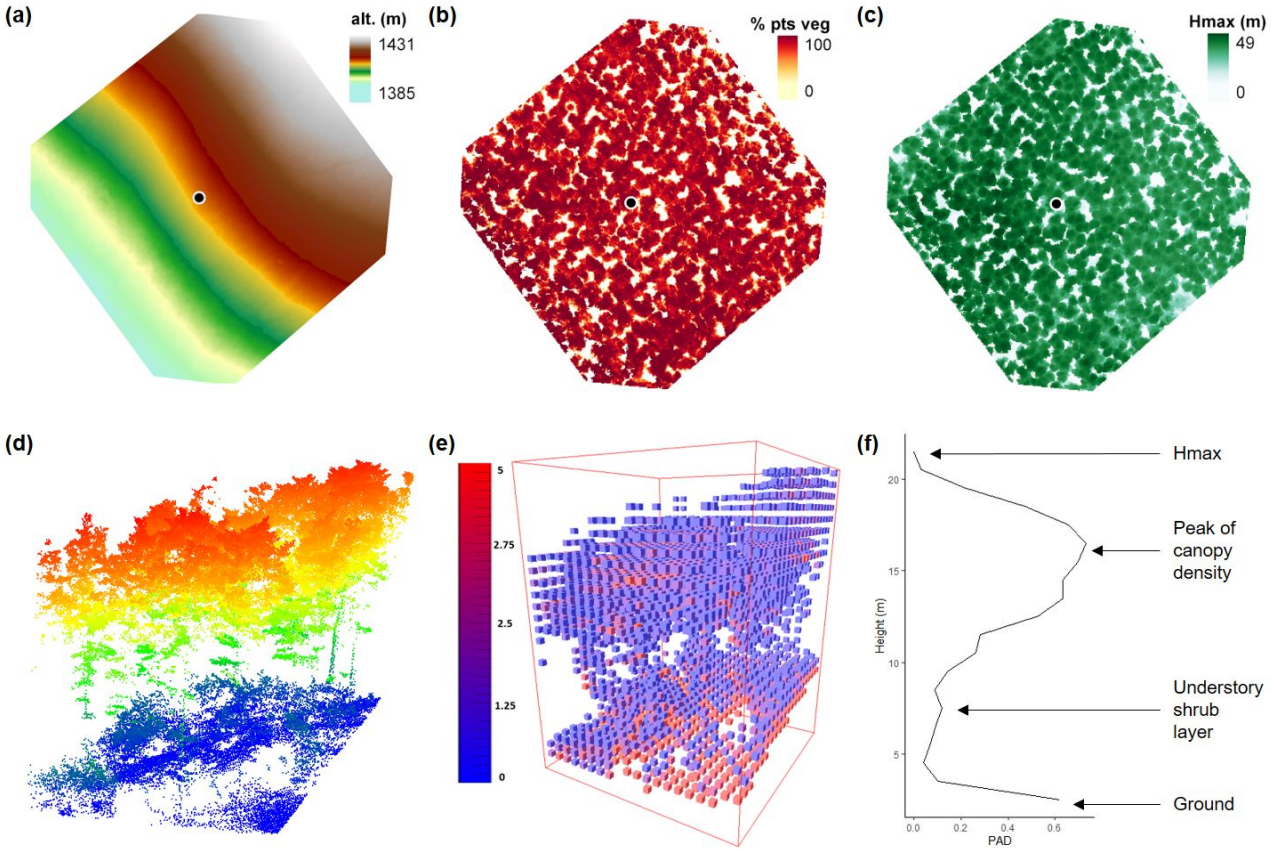

Fig. 3: Examples of LiDAR-derived variables to assess the vertical complexity below treetops. Upper panels (a, b, c): raster layers, at 50 cm × 50 cm resolution, showing the digital terrain model (DTM) (a), the percentage of points classified as "vegetation" (a proxy for canopy density) (b), and maximum canopy height (Hmax) (c) across a 0.5 ha area (ca. 70 m × 70 m) in the Aigoual forest (France). Lower panels (d, e, f): close-up on the raw 3D LiDAR point cloud across an area of 20 m × 20 m size (d) to derive plant or leaf area density (PAD or LAD) computed for small volume units or voxels of 50 cm × 50 cm × 50 cm size (e) further aggregated by height layer to generate a vegetation profile of PAD values (f). Data were acquired with a non-stationary ALS (YellowScan Vx20) (cf. **Fig. 2e**).

Figure 4

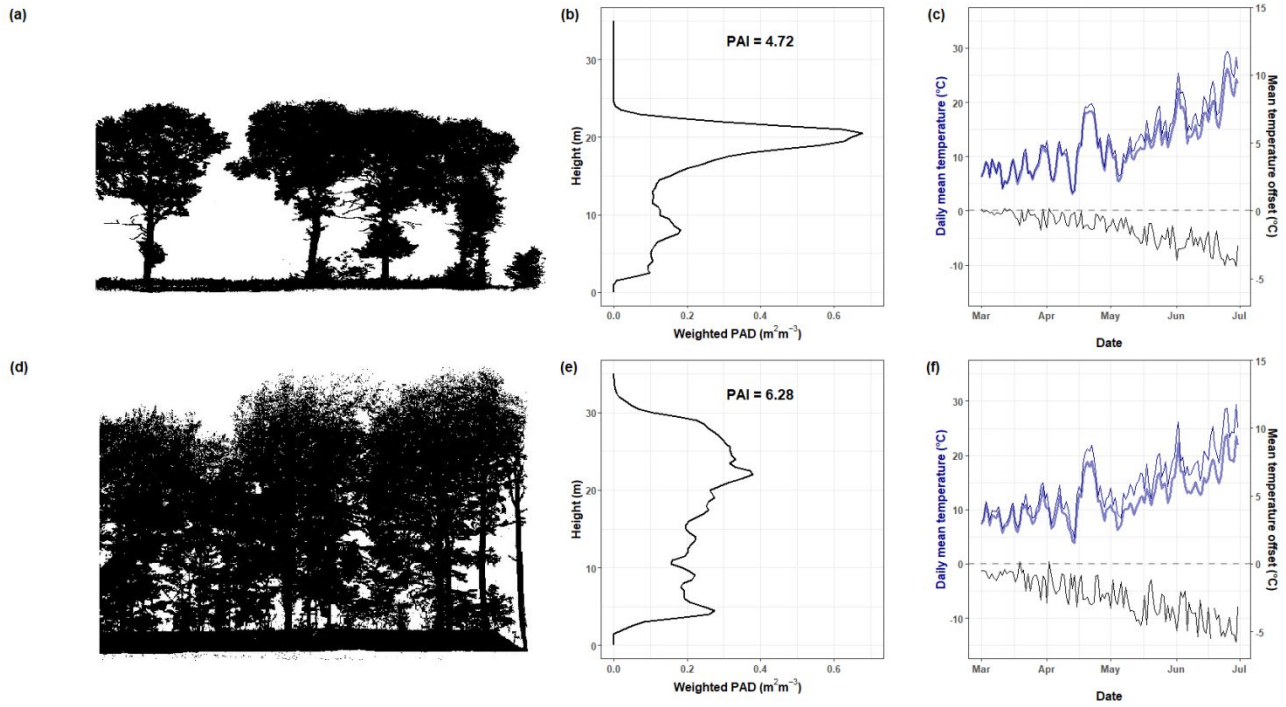

Fig. 4: Using terrestrial LiDAR systems (TLS) to derive variables explaining the variation in forest microclimates in an open (a, b, c) vs. dense (d, e, f) oak forest located in Belgium. Left panels (a, d): cross section of the raw lidar point cloud data. Central panels (b, e): vertical profiles of plant area density (PAD) (m^2 m^{-3}) values as a function of the height of the same point clouds used to compute the total plant area index (PAI), which is the integral of the PAVD-profile over the canopy height. Right panels (c, f): daily mean temperature (°C, blue lines) collected both inside (light-blue lines) and outside (dark-blue lines) the respective forest stands. The daily mean temperature offset, determined as the temperature inside the forest minus the temperature outside the forest, is shown in black as well. The LiDAR data was acquired using a RIEGL VZ400 (RIEGL Laser Measurement Systems GmbH, Horn, Austria). Single-scan position TLS was carried out in a dense and open forest in Belgium during the summer of 2018.

1157 **Figure 5**

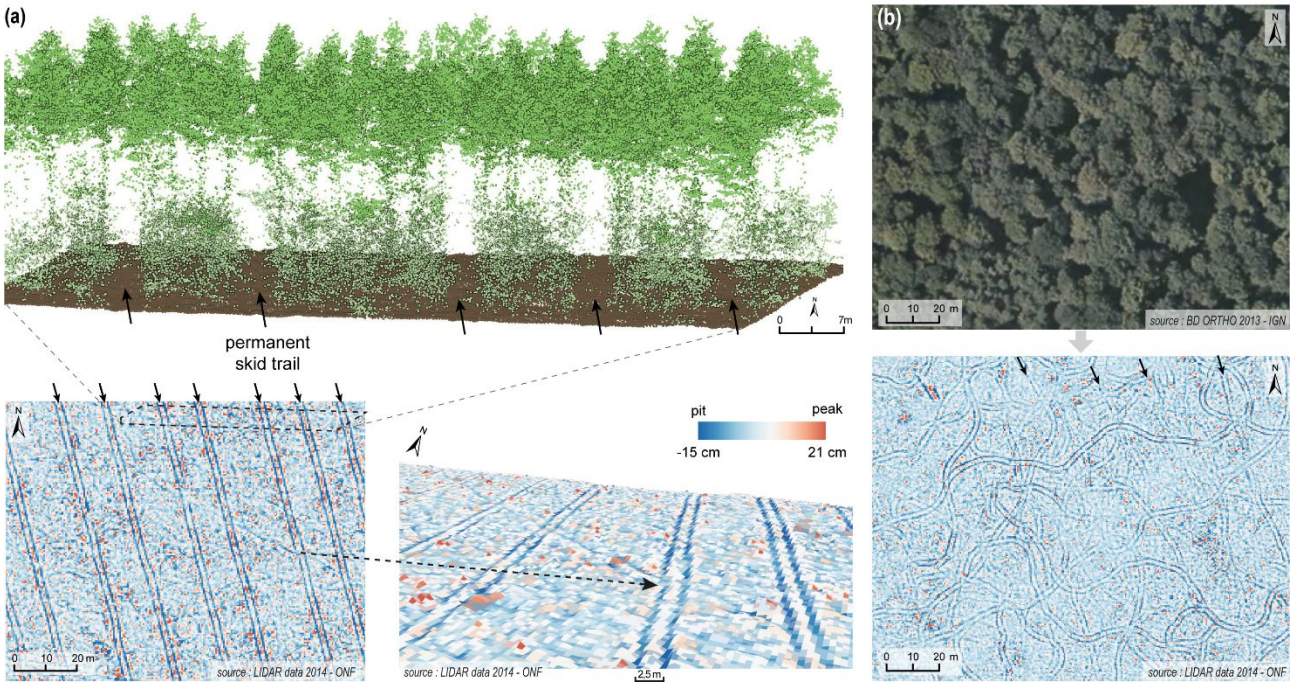

1158 **Fig. 5:** Using airborne LiDAR systems (ALS) to unveil regular (a) and irregular (b) skid trails below
1159 treetops. A local relief model (LRM), at 50 cm resolution, was derived from the digital terrain
1160 model (DTM) of the Compiègne forest in Northern France. Left panel (a): a 3D view of the raw
1161 LiDAR point cloud with regular skid trails, illuminated in dark blue colors by the LRM, below the
1162 canopy cover of a young forest stand. Right panel (b): irregular and meandering patterns of skid
1163 trails, likely from different ages, below the canopy cover of a more mature forest stand. Green and
1164 brown points represent points classified as vegetation and soil, respectively. Bluish and reddish
1165 colours in the LRM refer to the micro-variation of the terrain microrelief and represent hollows
1166 (ruts here) and bumps, respectively. The LiDAR data was acquired by the Office National des
1167 Forêts (ONF) across the entire lowland forest of Compiègne (144 km^2). The AERODATA Company
1168 used a Riegl LMS-680i LiDAR installed on-board an aircraft and performed flights in February 2014
1169 to get an average density of 12 points per m^2.

1170 **Figure 6**

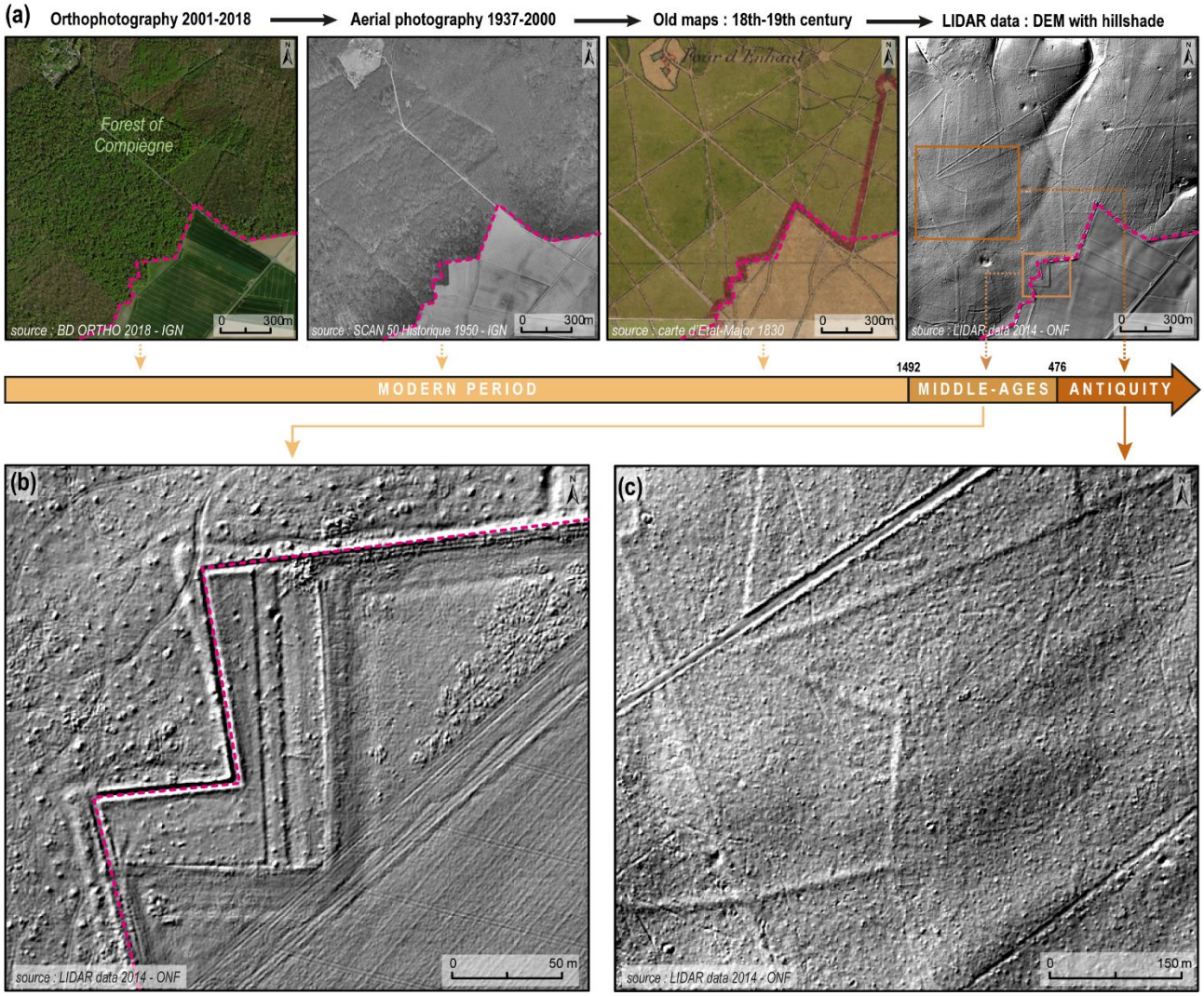

1171 **Fig. 6:** Using airborne LiDAR systems (ALS) to extend a chronosequence (a) and unveil past land
1172 uses (b, c). Upper panel (a): chronosequence of land uses at the southern edge of the Compiègne
1173 forest in Northern France reconstructed with the help of modern orthophotography, historical
1174 aerial photography, old archives from Cassini maps, and LiDAR data allowing us to extend the
1175 chronosequence until the Middle Ages and Antiquity. We used a digital terrain model (DTM), at 50
1176 cm resolution, with hillshade to unveil former agricultural practices inside the study area. The DEM
1177 with hillshade on the right-hand side of panel (a) clearly highlights artificial excavations (i.e., see
1178 the closed depressions) likely originating from the late Iron Age and Roman times and suggesting
1179 marling/liming practices to enrich agricultural fields. Bottom panels (b, c): close-up across two
1180 sites near the southern edge of the forest: evidence of (b) a typical late Middle Ages strip field

with cultivation ridges and (c) linear microreliefs corresponding to a network of Gallo-Roman agrarian fields and secondary roads. The LiDAR data was acquired by the Office National des Forêts (ONF) across the entire lowland forest of Compiègne (144 km^2). The AERODATA Company used a Riegl LMS-680i LiDAR installed on-board an aircraft and performed flights in February 2014 to get an average density of 12 points per m^2.

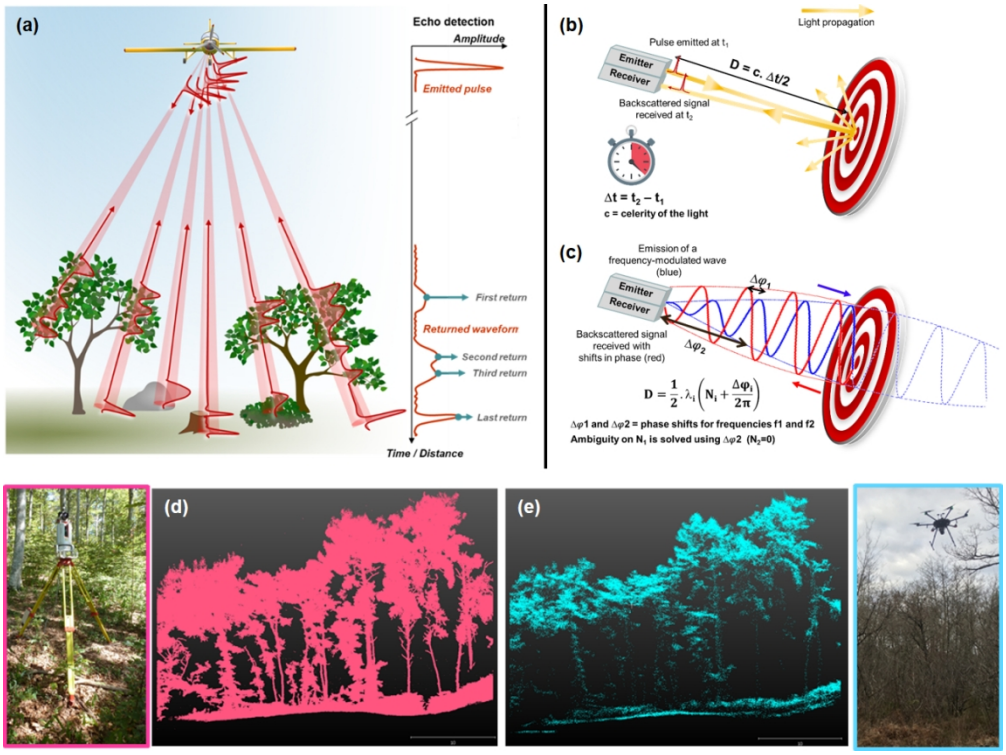

How light detection and ranging (LiDAR) works (a, b, c) and the mean to acquire LiDAR data from below or from above treetops (d, e). Upper-left panel (a): example of a non-stationary airborne LiDAR system (ALS) on board an aircraft. Upper-right panels (b, c): basic principles of time-of-flight vs. phase-shift LiDAR. Lower panels (d, e): data visualization of raw LiDAR point clouds extracted from both a stationary terrestrial LiDAR system (TLS) (Riegl VZ400) and a non-stationary ALS (YellowScan Vx20) covering the exact same study area in the Aigoual forest (France)

570x425mm (59 x 59 DPI)

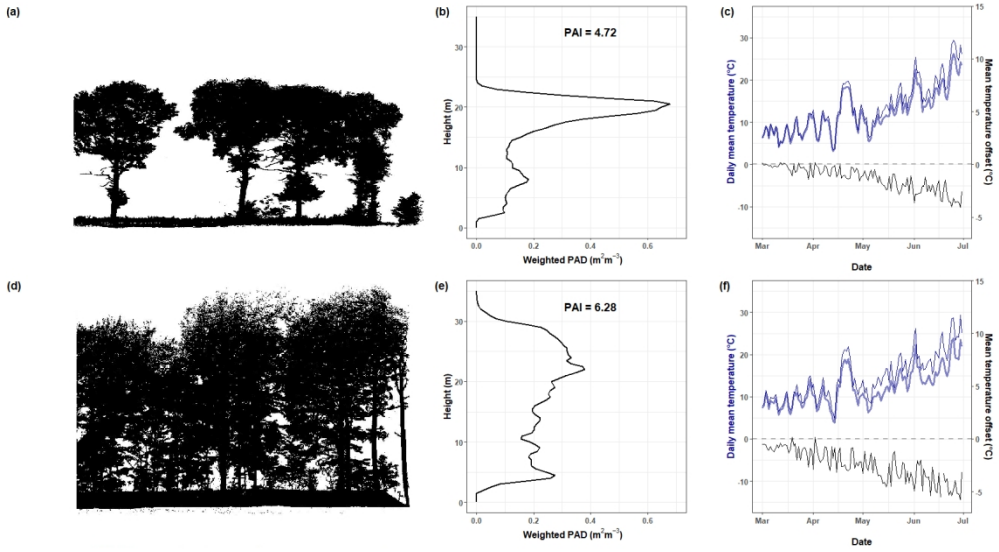

Using terrestrial LiDAR systems (TLS) to derive variables explaining the variation in forest microclimates in an open (a, b, c) vs. dense (d, e, f) oak forest located in Belgium. Left panels (a, d): cross section of the raw lidar point cloud data. Central panels (b, e): vertical profiles of plant area density (PAD) (m2 m−3) values as a function of the height of the same point clouds used to compute the total plant area index (PAI), which is the integral of the PAVD-profile over the canopy height. Right panels (c, f): daily mean temperature (°C, blue lines) collected both inside (light-blue lines) and outside (dark-blue lines) the respective forest stands. The daily mean temperature offset, determined as the temperature inside the forest minus the temperature outside the forest, is shown in black as well. The LiDAR data was acquired using a RIEGL VZ400 (RIEGL Laser Measurement Systems GmbH, Horn, Austria). Single-scan position TLS was carried out in a dense and open forest in Belgium during the summer of 2018

924x507mm (47 x 47 DPI)